

1 Exceptional loss in ozone in the Arctic winter/spring 2020

2 Jayanarayanan Kuttippurath^{1*}, Wuhu Feng^{2,3}, Rolf Müller⁴, Pankaj Kumar¹, Sarath Raj¹,
3 Gopalakrishna Pillai Gopikrishnan¹, Raina Roy⁵

4
5 ¹CORAL, Indian Institute of Technology Kharagpur, Kharagpur–721302, India.

6 ² National Centre for Atmospheric Science, University of Leeds, Leeds, LS2 9PH, UK

7 ³ School of Earth and Environment, University of Leeds, Leeds, LS2 9JT, UK

8 ⁴Forschungszentrum Jülich GmbH (IEK-7), 52425 Jülich, Germany

9 ⁵Department of Physical Oceanography, Cochin University of Science and Technology, Kochi, India

10
11
12 *Correspondence to:* Jayanarayanan Kuttippurath (jayan@coral.iitkgp.ac.in)

13
14 **Abstract.** Severe vortex-wide ozone loss in the Arctic would [expose both ecosystems and several millions of people](#) to
15 unhealthy ultra-violet radiation levels. Adding to these worries, and extreme events as the harbingers of climate change,
16 exceptionally low ozone with column values below 220 DU occurred over the Arctic in March and April 2020. Sporadic
17 occurrences of low ozone with less than 220 DU at different regions of vortex for almost three weeks were found for the first
18 time in the observed history in the Arctic. Furthermore, a large ozone loss of about 2.0–3.4 ppmv triggered by an unprecedented
19 chlorine activation (1.5–2.2 ppbv) matching the levels occurring in the Antarctic was also observed. The polar processing
20 situation led to the first-ever appearance of loss saturation in the Arctic. Apart from these, there were also ozone-mini holes in
21 December 2019 and January 2020 driven by atmospheric dynamics. The large loss in ozone in the colder Arctic winters is
22 intriguing, and demands rigorous monitoring of the region.

23 **1 Introduction**

24 Apart from its significance of shielding the harmful ultra-violet (UV) radiation reaching the surface of earth, stratospheric
25 ozone is a key component in regulating the climate (e.g. Riese, et al., 2012). Changes in stratospheric ozone are always a big
26 concern for both public health and climate (WMO, 2018; Bais et al., 2019). Due to unbridled emissions of Ozone Depleting
27 Substances (ODS) to the atmosphere since the 1930s stratospheric chlorine peaked in the polar stratosphere in the early 2000s
28 (Newman et al., 2007; Engel et al., 2018; WMO, 2018). The first signatures of polar ozone loss appeared over Antarctica by
29 the late 1970s (Chubachi et al., 1984; Farman et al., 1985), and it peaked to saturation levels in the late 1980s [due to already](#)
30 [high levels of stratospheric chlorine](#) (Kuttippurath et al., 2018). Recent studies have demonstrated the effectiveness of Montreal
31 Protocol and its amendments and adjustments in reducing halogen gases, with a corresponding positive trend in ozone in
32 Antarctica (Salby et al., 2011; Kuttippurath et al., 2013; Solomon et al., 2016; Chipperfield et al., 2017) and in northern mid-

33 latitudes (Steinbrecht et al., 2014; Nair et al., 2015; Weber et al., 2018). However, a positive trend in the Arctic ozone is not
34 reported yet possibly because of the large dynamically driven inter-annual variability of ozone there (Kivi et al., 2013; WMO,
35 2018).

36

37 Antarctic winters are very cold and the ozone hole is a common feature of these winters since the late 1970s. There were
38 winters with very low stratospheric temperatures with a stronger vortex that showed relatively larger loss in ozone, such as the
39 winters of 1996, 2000, 2003, 2006 and 2015 (Bodeker et al., 2005; Chipperfield et al., 2017). There were also winters with
40 high temperatures and smaller ozone losses as in the case of 1998, 2002, 2012 and 2019 (Müller et al., 2008; de Laat et al.,
41 2010; Kuttippurath et al., 2015). Yet, the inter-annual variability of ozone loss in the Antarctic is very small in recent decades.
42 On the other hand, colder winters with large losses of ozone (e.g. > 1.5 ppmv of loss) are rare in the Arctic (Rex et al., 2015, von
43 der Gathen et al., 2021). The ozone loss derived from satellite and ozonesonde measurements show that most winters have
44 ozone loss in the range of 0.5-1.5 ppmv and extremely cold winters showed large loss of about 1.5–2.0 ppmv (Manney et al.,
45 2003; Kuttippurath et al., 2013; Livesey et al., 2015). Similarly, the ground-based measurements show about 15–20% of loss
46 in most Antarctic winters, but the winters 1995, 1996, 2000, 2005 and 2011 were very cold with large loss of ozone, up to 25–
47 30% (Goutail et al., 2005; Pommereau et al., 2018). However, these ozone loss values are still smaller than the 40–55% loss
48 occurrence in the Antarctic (Kuttippurath et al., 2013; Pommereau et al., 2018).

49

50 The Arctic vortex is relatively short-lived (i.e. three to four months). The vortex normally strengthens by mid-December or
51 early January and dissipates by mid-March. Major and minor warmings are common features of Arctic winters. The Arctic
52 vortex in any winter would be frequently disturbed by planetary waves that emanate from the troposphere. In general, planetary
53 wave numbers 1, 2 and 3 are mostly responsible for the momentum transfer to the stratosphere. This dynamical activity would
54 increase the temperature in the lower stratosphere and trigger stratospheric warmings. The warmings can be minor or major,
55 depending on the strength of wave activity, increasing the polar temperature and eventually disturbing the polar vortex. The
56 vortex can be distorted, displaced, elongated and even split in two in accordance with the potency of momentum imparted by
57 the waves. When the polar vortex is disturbed, the ozone loss will be smaller and the final warming can be as early as in late
58 February or early March, as for many Arctic winters (e.g. Manney et al., 2003; Kuttippurath et al., 2012; Goutail et al., 2015).
59 However, the vortex dissipates and chemical ozone loss terminates when a major warming occurs there. In an earlier study,
60 Kuttippurath et al. (2012) observed an increasing trend in major warmings, and ozone loss is found to be proportional to the
61 timing of the major warmings, as early winter warmings stop polar stratospheric cloud (PSC) formation (i.e. stop the action of
62 heterogeneous chemistry) because of the higher temperatures. This situation limits the activated chlorine available for ozone
63 loss and results in smaller loss in warm Arctic winters. Since 1979, during the satellite era, there were two extreme winters
64 with large loss of ozone in the Arctic; 2005 and 2011 (Coy et al., 1997; Feng et al., 2007; Horowitz et al., 2011). The occurrence
65 of extreme events is a feature of climate change (e.g. IPCC, 2007). Therefore, the extremely cold winters with large loss in
66 ozone could also be a harbinger of climate change. Previous studies have postulated that the cold winters will get even colder

67 with large loss in ozone (Sinnhuber et al., 2000; Rex et al., 2004; Chipperfield et al., 2005; Rider et al., 2013, von der Ga then
68 et al., 2021). Analyses of the past colder Arctic winters indicate that it is likely that the colder winters may experience large
69 loss in ozone, as in the case of 2005, 2016 and 2011. There are already studies on this winter discussing the ozone loss and
70 meteorology (Manney et al., 2020; Wholtmann et al., 2020; Rao and Grafinkel, 2020; Weber et al., 2021; Innes et al., 2021;
71 Wilka et al., 2021; Grooß and Müller, 2021; von der Gathen et al., 2021; Feng et al., 2021). However, in this study, we use
72 different data sets, different loss estimation methods, and several assessment parameters together to study the polar processing
73 and ozone loss in the Arctic winter 2020, and such an analysis is never done for this winter. This is particularly important as
74 the winter was very cold with the largest ozone loss in the observational record and experienced the total column ozone (TCO)
75 values below 220 DU for several days in the vortex, for the first time.

76 **2 Data and Methods**

77 We have used two satellite ozone profile datasets. The level 2 data from the

- 78 (i) Microwave Limb Sounder (MLS) v4.2 and
- 79 (ii) Ozone Mapping and Profiler Suite (OMPS) v2.5 (ozone).
- 80 (iii) We have also used the ozonesonde measurements from the Arctic stations at Alert (62.34° N, 82.49° W) and Eureka
81 (79.99° N, 85.90° W). The ozonesonde measurements have an uncertainty of 5–10% (Smit et al., 2007).

82

83 Three satellite-based total column ozone (TCO) data are also employed (level 3) for our analyses

- 84 (iv) Ozone Monitoring Instrument (OMI, DOAS v003),
- 85 (v) OMPS (v2.1),
- 86 (vi) Global Ozone Monitoring Experiment (GOME) 2 (GDP4.8),
- 87 (vii) Modern-Era Retrospective analysis for Research and Applications (MERRA)-2 and
- 88 (viii) Brewer spectrometers from Alert and Eureka.

89

90 These TCO measurements have an uncertainty of 2–5%. The ozone and other trace gas profiles are provided in pressure
91 coordinates, which are converted to isentropic coordinates using the temperature data from the same satellite, except for OMPS,
92 for which the temperature data are taken from ERA5. We use the European Centre for Medium-Range Weather Forecasts
93 (ECMWF) Reanalyses ERA5 potential vorticity (PV) on a 1°×1° grid to determine the vortex edge. The PV data are also
94 converted to isentropic coordinates using the ERA5 temperature data. We computed the equivalent latitude at each isentropic
95 level at 5 K intervals from 350 to 800 K, which is then used to compute the vortex edge using the Nash et al. (1996) criterion.
96 We use measurements inside the polar vortex for the ozone loss analysis. The missing values in satellite measurements were
97 filled with linear interpolation.

98

99 We have taken ozone, ClO, HNO₃ and N₂O from the Aura MLS measurements. The ozone measurements at 240 GHz have a
100 vertical resolution of 2–3 km, vertical range of 261–0.02 hPa and an accuracy of 0.1–0.4 ppmv. The vertical range of HNO₃
101 measurements is 215–1.5 hPa, vertical resolution is 2–4 km, with an accuracy of 0.1–2.4 ppbv, depending on altitude. The
102 N₂O measurements are available for the 68–0.46 hPa vertical range, and 68 hPa roughly equivalent to the 400 K isentropic
103 level. The data were extrapolated up to 350 K by performing exponential fitting to N₂O vertical distribution at 400–600 K by
104 considering the exponential change of N₂O with altitude. The accuracy of retrievals at 190 GHz is about 2–55 ppbv at this
105 altitude range and the vertical resolution is about 2.5–3 km. The vertical resolution of ClO measurements at 640 GHz is about
106 3–3.5 km over 147–1 hPa, and the accuracy of measurements is about 0.2–0.4 ppbv. The measurements also have latitude-
107 dependent bias of about 0.2–0.4 ppbv, depending on altitude (Livesey et al., 2013; Santee et al., 2008; Froidevaux et al., 2008).

108

109 The OMPS consists of three sensors that measure scattered solar radiances in overlapping spectral ranges and scan the same
110 air masses within 10 min. The nadir measurements are used to retrieve ozone total column and vertical profiles (NP). The
111 Limb Profiler (LP) measures profiles with high vertical resolution (~ 2–3 km) and the LP retrievals are in good agreement
112 with other satellite measurements and the differences are mostly within 10% (Kramarova et al., 2018). The OMPS TCO shows
113 0.6–1.0% differences with Brewer and Dobson ground-based TCO measurements across the latitudes, and are also biased +2%
114 when the TCO is above 220 DU (Bais et al., 2014). GOME-2 was flown on MetOp-A satellite in 2006. The GOME-2 ozone
115 column has a positive bias in the northern high latitudes of about 0.5–3.5% (Layola et al., 2011). The OMI TCO measurements
116 have an accuracy of about 5% in the polar regions (Kroon et al., 2008; Kuttippurath et al., 2018). The Brewer spectrometers
117 operate in the UV region and their ozone observations have an accuracy of about 5%.

118

119 The ozone loss is estimated using two different methods and four different datasets to make sure the analyses are robust. The
120 first method used is the widely used profile descent method, wherein the N₂O data are used for the calculations of air mass
121 descent in the polar vortex. The reference profile of N₂O was taken from the month of December, and therefore, the loss
122 calculations are presented from December (May for Antarctic) onwards. The second method used for the calculation of ozone
123 is the passive tracer method, for which a passive odd-oxygen tracer is simulated using a CTM (Chemical Transport Model)
124 and is subtracted from the measured ozone to determine the ozone loss, as the changes in tracer are modulated only by the
125 dynamics (Feng et al., 2005). We have used the SLIMCAT model for the tracer calculations (Chipperfield, 2006) and
126 investigated the Arctic ozone loss under different meteorological conditions including Arctic winter/spring 2020 (e.g.,
127 Chipperfield et al., 2005; Bognar et al., 2021; Feng et al., 2021; Weber et al., 2021).

128 3. Results and discussion

129 3.1 The exceptional meteorology of the Arctic winter/spring 2020

130 Figure 1 shows the times series of stratospheric meteorology in the Arctic winter/spring 2020 compared to that [long-lasting](#)
131 [polar vortex](#) years 1997 and 2011. Time series of the meteorological parameters for all Arctic winters [since 1979](#) are also
132 [shown](#) (grey coloured curves) for comparison. In general, the temperatures are between 210 and 195 K. In 2020, the
133 temperatures were about 195 K in December, 190–195 K in January–March and 195–205 K in April. [However, the minimum](#)
134 [temperature in late winter 2020](#) is generally lower than 195 K, lasting about 115 days from December through early April. The
135 temperatures are general lower than those in the 2011 winter, and those in late March and April are the lowest on the
136 observational record. [The lower temperatures in late December through mid-March](#) are key to PSCs, chlorine activation, [the](#)
137 [maintenance of high values of active chlorine and ozone loss](#). Low temperatures are thus a common phenomenon in winters
138 with large loss of ozone (e.g. 1995, 2000, 2005 and 2011). [Therefore, the higher temperatures in early winter and limited](#)
139 [chlorine activation were the reason for relatively smaller ozone loss in 1997](#); although it was a winter with a strong vortex up
140 [to the end of April](#) (Coy et al., 1997; Feng et al., 2007; Kuttippurath et al., 2012). Since minor warmings (mWs) are very
141 common in the Arctic winters, we also examined the occurrence of mW events by [checking the temperature at 90° \(North](#)
142 [Pole\) and 60° N at 10 hPa and zonal winds at 60° N at 10 hPa](#). The analyses show a small increase in temperature on 5 February
143 2020 (i.e. a minor warming) and a corresponding change in zonal winds.

144
145 The temperatures were consistently lower than the nitric acid trihydrate (NAT) equilibrium threshold of about 195 K and
146 therefore, large areas of Polar Stratospheric Clouds (PSCs) are observed from December to mid-February. Even though PSCs
147 may also be composed of liquid particles and not only NAT (e.g. Pitts et al. 2009; Spang et al., 2018), the NAT equilibrium
148 threshold constitutes a good estimate for the occurrence of heterogeneous chemistry (e.g. Groöß and Müller, 2021; von der
149 Gathen et al., 2021). The [potential PSC area \(APSC\)](#) was about 4 million km² in December 2020 at 460 K, but it doubled in
150 January through mid-March. The APSC from mid-February to late March is also largest on the observational record (Figure
151 1). The low temperatures (i.e. lower than 188 K) also produced a very high amount of ice PSCs at the end of January and early
152 February (up to 4 million km²) when the lowest temperatures [in 40 years were recorded in the Arctic](#). This is the [largest ice](#)
153 [PSC ever observed in terms of its area, volume and number of days of appearance \(i.e. frequency\)](#) in the Arctic and the area is
154 twice that of the winter 2011 ([also see Deland et al., 2020](#)). The PSC area shrunk to half of its area in late January and February,
155 as the lower stratospheric temperature increased during the period. This was the only occasion that the temperature increased
156 and PSC areas limited to below 4 million km² in the winter 2020. Note that the PSC area and volume were largest in 2016, not
157 in 2020 (Figure S1) (Kirner et al., 2015).

158
159 The potential vorticity (PV) at ~17 km (about 460 K potential temperature level) show that the polar vortex was very strong
160 in the lower stratosphere in 2020. The PV values were consistently higher than the previous cold (i.e. 1995, 2000, 2005 and

161 2011) and long lasting (e.g. 1997 and 2011) winters in March and April. This indicates that the winter 2020 had the strongest
162 vortex in the recent history, as demonstrated by the PV time series of different Arctic winters (Figure 1, second panel, left).
163 However, the zonal winds were strongest in 1997 during the March-April period. [The diagnosis with heat flux and the eddy](#)
164 [heat flux associated with waves demonstrates that the momentum transported from the troposphere to stratosphere was very](#)
165 [weak in 2020 \(in the range of \$-20\$ to \$30 \text{ Km s}^{-1}\$ \), and the heat flux values are zero or negative \(e.g. \$-10 \text{ Km s}^{-1}\$ in February\)](#)
166 [during most part of the winter. These results are also in agreement with the eddy heat flux computed for the waves, as they](#)
167 [also show smaller wave momentum to the stratosphere. In short, the eddy heat flux and wave heat flux show smaller values in](#)
168 [January-April; indicating the reason for the less disturbed long-lasting vortex in 2020. According to Lawrence et al. \(2020\),](#)
169 [apart from the weak tropospheric forcing, the formation of reflective configuration of stratospheric circulation was another](#)
170 [factor that aided in the strengthening of the vortex in 2020.](#)

171

172 The potential vorticity analyses show a strong and large vortex in early December. The vortex began to grow and occupied the
173 entire polar region (defined by PV vortex edge) by early January, as shown in Figure 2. The lowest temperatures of the past
174 40 years were recorded by the end of January and the vortex was exceptionally strong and large (e.g. [Wohltmann et al., 2020;](#)
175 [Rao and Garfinkel, 2020](#)). The mW distorted and elongated the vortex in early February, but the vortex was still strong and
176 continued to be intact until the last week of April 2020. The extraordinary persistence of a strong and undisturbed Arctic vortex
177 in March and April is evident in the PV maps. [We also examined the Arctic winters since 1979 in terms of their dynamical](#)
178 [activity, as shown in Figure S1b. The analyses show that, although the average vortex temperature and vortex area at 70 hPa](#)
179 [was not very exceptional, the westerly winds \(\$25 \text{ ms}^{-1}\$ \) were strongest and dynamical activity was weakest \(with heat flux \$17\$](#)
180 [K \$\text{ms}^{-1}\$ \) in the past twenty years. This further suggests that the winter 2020 was unique and that wave forcing was very weak](#)
181 [during the period.](#)

182 **3. 2 Strong air mass descent and associated ozone distribution**

183 Figure 3 shows the distribution of ozone, ClO, N₂O, HNO₃ and the ozone loss estimated for the winter 2020 using satellite
184 observations. [We use the measurements from MLS on the Aura satellite \(Livesey et al., 2015\). The MLS data has been widely](#)
185 [used for the study of polar ozone loss, as the instrument provides measurements of some key ozone-related chemistry trace](#)
186 [gases such as ClO, N₂O and HNO₃ to delineate the features of chlorine activation, vortex descent and denitrification,](#)
187 [respectively \(Manney et al., 2020\). The ozone distributions in the vortex show \$< 1.0\$ ppmv in December, slightly higher values](#)
188 [of about 1.5 ppmv in February and smaller than 1.0 ppmv from Mid-March to the end of April at 400 K. The measurements](#)
189 [show exceptionally low values of ozone, about 0.5 ppmv or below, during the period mid-March through to the end of April](#)
190 [at 350–450 K. The ozone values show \$< 2.5\$ ppmv from December to mid-January, \$< 2\$ ppmv January and February and \$< 1.0\$](#)
191 [ppmv in March-April at 350–450 K, and about 2–4 ppmv above 500 K; suggesting an unusual chemical depletion of ozone in](#)
192 [December and late January. The ozone values are about 3–4 ppm above 550 K throughout the winter; implying little reduction](#)
193 [in ozone there. The unusual feature here is the extremely small ozone mixing ratios of 1.0 ppmv in early December and March–](#)

194 April below 450 K (about 16 km). This reveals huge depletion of ozone in the lower stratosphere and therefore, we have
195 quantified the ozone loss for the winter. [We use the profile descent method using the trace of air motions N₂O and is a widely](#)
196 [used method for ozone loss estimation \(Bremer et al., 2002; Rex et al., 2002; Jin et al., 2006\).](#)
197

198 For instance, the MLS measurements show that N₂O values were 250 ppbv at 400 K, 150 ppbv at 500 K and 50 ppbv at 600
199 K in December. The N₂O observations show strong air mass descent with values down to 100 ppbv at 400 K and about 25–50
200 ppbv above 500 K in early February. Again, N₂O values exhibit below 50 ppbv in late March at 400 K. The N₂O distributions
201 show below 50 ppbv at all altitudes from early February onwards; suggesting substantial dynamic descent in the stratosphere.
202 When a particular altitude is considered, e.g. the 450 K potential temperature level, the N₂O values show 160 ppbv in early
203 December, 100 ppbv in early January, 50 ppbv in early February and less than 50 ppbv thereafter. On the other hand, the N₂O
204 distributions show 50 ppbv in early December and below that value afterwards at 500 K. The severe air mass descent in this
205 winter is further depicted in Figure S2, where monthly correlations between ozone [and](#) N₂O are presented.

206 **3.3 Ozone loss and mini-holes in December and January**

207 [There were vortex-wide PSC occurrences in the first week of December](#), about 2-4 million km² in area (APSC) and about 70
208 million km³ in volume (VPSC) ([see Rex et al., 2005 for their definitions](#)). The APSC and VPSC dropped significantly
209 afterwards and then gradually increased again by mid-December to 10 and 120 million km³, respectively. An unusual increase
210 in activated chlorine is observed during the first week of December in conjunction with the appearance of PSCs. The
211 temperatures began to decrease from 198 K in mid-December to 187 K by the end of January, as shown in Figure 1. The
212 chlorine activation peaked and showed record levels of ClO, about 1.5–2.0 ppbv at 400–600 K, during this period. The
213 chemical ozone loss began in early January with about 0.5 ppmv and increased to 1.5 ppmv by the end of January below 500
214 K. The loss above that altitude is always lower than 0.5 ppmv, which shows that the ozone loss is restricted to the altitudes
215 below 21 km (i.e. 550 K).

216
217 In general, [the ozone loss starts in December in the middle stratosphere and then gradually progresses towards the lower](#)
218 [stratosphere by January](#). The loss would be below 0.5 ppmv in December and about 0.5–1.0 ppmv in January in the lower
219 stratosphere in cold Arctic winters. However, in the Arctic winter 2020, the ClO and ozone loss show unusually high values
220 of about 1.5–2.0 ppbv and 1.5–2.0 ppmv, respectively. [Since ozone loss of this scale requires sunlight and high levels of ClO,](#)
221 [and there is no sunlight in the Arctic vortex in early winter](#), the appearance of huge amounts of ClO during this period is
222 surprising. The only possibility to have such high-levels of chlorine activation is the displacement of vortex to sunlit latitudes.
223 The analyses of vortex position in early December and late January (Figure 2) reveal that the vortex was at 55°–60° N.
224 Therefore, a strong polar vortex, very low temperatures, large volumes of PSCs and shift of vortex to the sun light part of mid-
225 latitudes caused the unprecedented chlorine activation and ozone loss in the first week of December and late January. This is
226 similar as Arctic winter 2002/03 (e.g. Goutail et al., 2005; Kuttippurath et al., 2011).

227

228 In addition to the ozone loss inside the vortex, there is another interesting phenomenon in December and January. The analyses
229 of TCO show that there were Arctic ozone mini-holes (e.g. Stenke and Grewe, 2003; Rieder et al., 2013) of about 300–700
230 km² size in the first week of December (1–6 December 2019) and on 26 January 2020 (Figure 4). The lowest TCO measured
231 of the winter was also at the latter date. A detailed analysis with TCO, PV, temperature and ClO reveal that those ozone mini-
232 holes were dynamically driven, as there was rapid air mass transport to the southern Arctic in early December and late January.
233 These ozone mini-hole occurrences due to rapid changes in weather patterns and the total column ozone returns to the amount
234 of normal levels of ozone in few days

235

236 Ozone mini-holes are a dynamically driven sporadic decrease in TCO observed mostly in the mid-latitudes of both hemispheres
237 due to rearrangement of the ozone column associated with tropospheric weather systems (Reed, 1950). The mini-holes are
238 called so, as the TCO is less than 220 DU in those areas, and is one of the criteria defining the Antarctic ozone hole, although
239 they differ in the nature of formation and spatial extent. These transient spatial and temporal events were identified first by
240 Dobson and Harrison (1926) much before the identification of chemical ozone loss and were referred to as mini-holes by
241 Newman et al. (1988) and McKenna et al. (1989). The plunge in TCO results when, the horizontally advected ozone poor
242 tropospheric air mass interacts with the vertical air column motions in the anticyclonic ridging regions of the upper troposphere
243 in the polar regions. As a consequence of this divergence, mixing or both may result in the appearance of mini-holes (e.g.
244 Peters et al., 1995; James et al., 1997; Canziani et al., 2002). Since its identification, the criteria for the definition of mini-holes
245 differed based on the thresholds of TCO amounts and spatial coverage in different geographical locations (Millán and Manney,
246 2017). In our study the threshold is taken to be 220 DU (see Bojkov and Balis, 2001). Many studies have also analysed the
247 mini-hole formations in the northern hemisphere (e.g. James, 1998; Krzyścin, 2002; Stenke and Grewe, 2003; Feng, 2006).
248 Here, we analyse the ozone mini-holes that appeared in the polar region of the winter 2020 and their dynamical origin.

249

250 We used the HYSPLIT trajectory model to find the air mass transport at three different altitudes (17, 18 and 19 km) in the
251 lower stratosphere, where the mini-holes are found (Figure 4, right panels). The air mass exported from mid- and low latitudes
252 has very low PV values, low temperature and high ClO. It suggests that the TCO transported from mid-latitudes triggered the
253 ozone “holes” (ozone values < 220 DU). To further examine the low ozone values outside the vortex, we selected two
254 ozonesonde measurements in the region (Alert: 62.34° N, 82.49° W and Eureka: 79.99° N, 85.90° W), which are shown in
255 bottom panels of Fig. 4 for selected dates in December and January. These measurements show significant reduction in ozone
256 (Coy et al., 1997; Feng et al., 2007; Horowitz et al., 2011) between 12 and 18 km; confirming the findings from the satellite
257 total column measurements.

258

259 It should be mentioned that there was already large chemical loss of ozone inside the Arctic vortex in early December and late
260 January owing to the conventional polar ozone loss chemistry (as shown in Figure 3). However, the ozone mini-holes that

261 appeared outside the vortex were primarily caused by dynamics. We cross-checked TCO from OMI (Bias et al., 2014), OMPS
262 (Flynn et al., 2014), GOME-2 (Layola et al., 2011) and MERRA-2 (Gelaro et al., 2017), and found that the ozone mini-holes
263 were present in all these TCO datasets.

264 **3.4 Prolonged chlorine activation and chemical ozone loss**

265 When the Arctic winters are very cold, chlorine activation occurs in the Arctic lower stratosphere at 400–500 K in January and
266 February. In 2011, the chlorine activation was observed up to the end of February and was intermittent with a peak value of
267 about 1.6 ppbv, and was mostly at 400–500 K (e.g. Manney et al., 2011; Kuttippurath et al., 2012; Livesey et al., 2015; Griffin
268 et al., 2018). Conversely, in the Arctic winter 2020, there was continuous and sustained chlorine activation from December to
269 early April, except during the mW periods of mid-December and early February. The ClO values are also 0.5 ppbv larger than
270 those observed in the winter 2011. Feng et al. (2021) also stated that the chlorine activation in 2020 lasted longer than that in
271 2010/11. Therefore, strong chlorine activation was observed in March–April with ClO values of about 1.0–1.6 ppbv at 400–
272 550 K and the peak ClO value is about 2.1 ppbv.

273
274 The minor warming (Figure 1) caused a break in chlorine activation (Figure 3 for ClO) in early March. Nevertheless, the
275 temperature decreased shortly thereafter, which produced continued chlorine activation until early April at 400–550 K. The
276 ozone loss deepened in March and peaked by the end of March, and showed the maximum of about 1.5–3.4 ppmv at a broader
277 altitude range, up to 500 K. The ozone loss above that altitude (i.e. 550 K) was about 0.5–1 ppmv, which is still larger than
278 that of any other Arctic winter. In fact, the loss of 1.0 ppmv is the peak loss observed in normal or moderately cold winters
279 of the Arctic (e.g. Kuttippurath et al., 2013); suggesting the severity of ozone loss even at the higher altitudes in this winter.
280 The maximum loss in 2020 was recorded at the end of March to the end of April, about 2.0–3.4 ppmv at 400–500 K and about
281 0.5–1.5 ppmv at 500–600 K. Furthermore, when compared to the early winter values, the late winter low HNO₃ values suggest
282 very severe denitrification, about 2–4 ppbv in the same period at 350–450 K (e.g. Manney et al., 2020). The HNO₃ values in
283 the lower stratosphere in March–April are about 60–80% lower than those of December–February at the same altitude levels
284 (Pommereau et al., 2018; Lindenmaier et al., 2012). The gravest denitrification was in December, with values of about 0–2
285 ppbv below 400 K and 4–6 ppbv at 400–450 K. Therefore, high chlorine activation and strong denitrification (as deduced from
286 the HNO₃ analyses shown in Figure 3) provided the basis for an unprecedented situation for large ozone loss of about 2–3.4
287 ppmv in the lower stratosphere in March–April.

288
289 Since the ozone loss in 2020 is exceptionally larger, we have employed another set of measurements to estimate ozone loss to
290 reconfirm that the derived results are robust. The loss estimated from OMPS measurements together with other analyses are
291 shown in Figure 5 (left). The maximum ozone loss profile extracted from the OMPS data shows very good agreement with
292 that from the MLS measurements for the Arctic winter 2020. The peak ozone loss values show about 2–2.8 ppmv in the lower
293 stratosphere below 550 K. Since the maximum ozone loss profiles are averaged for a few days, the loss values are slightly

294 lower than those from MLS. The lower stratosphere shows similar ozone loss values, but the loss above 500 K shows slightly
295 smaller values (0.1–0.5 ppmv) due to the low bias of OMPS measurements at these altitudes as compared to the MLS
296 measurements (Kramarova et al., 2018). The comparison with OMPS confirms that the method adopted for ozone loss is
297 robust. Our estimates are in good agreement with those of Manney et al. (2020), Weber et al. (2021) and Wohltmann et al.
298 (2020), who also derive a loss of about 2.1–2.8 ppmv below 450 K from the MLS measurements.

299 **3. 5 The Arctic ozone loss in the context of other Arctic winters**

300 Arctic winters are normally warmer than those in the Antarctic and occurrences of PSCs are sparse and infrequent. [Therefore,](#)
301 [high chlorine activation and significant ozone loss is limited to winters with very low temperatures in December–February](#)
302 (Tilmes et al., 2014; Goutail et al., 2005; WMO, 2018; Newman et al., 2008; Kuttippurath et al., 2012). The ozone loss observed
303 in warm winters (e.g. 2006 and 2009) is about 0.5–0.7 ppmv, moderately cold winters (e.g. 2008 and 2010) is about 1.0–1.2
304 ppmv and very cold winters (e.g. 2005) is 1.4–1.6 ppmv (e.g. WMO, 2018). However, the ozone loss in the winter 2011 was
305 about 1.0 ppmv (or 30–40 DU) larger [than that of other Arctic winters \(about 2.1–2.3 ppmv or 100–100 DU\). This ozone loss](#)
306 [was similar to the loss](#) found in warmer, more perturbed Antarctic winters (e.g. 1988 and 2002) (Manney et al., 2011;
307 Kuttippurath et al., 2012; Feng et al., 2015; Pommereau et al., 2018). We applied the same loss estimation method to the
308 measurements for the Arctic winter 2011 to compare with that of the Arctic winter 2020. This would also test the veracity of
309 the loss estimation procedure and the results are shown in Fig. 5.

310

311 The peak ozone loss in the Arctic winter 2011 is about 2.1 ppmv, which is in very good agreement with all other available
312 analyses for that winter (WMO, 2014, 2018; Griffin et al., 2018; Livesey et al., 2015). However, the ozone loss in the Arctic
313 winter 2020 is about 0.7 ppmv higher than that in 2011, about 2.8 ppmv. The difference in ozone loss between the winters is
314 negligible above 480 K. Therefore, it is evident that the ozone loss in the Arctic winter 2020 is the largest on the record and is
315 significantly higher than that of any previous Arctic winter. A very [similar conclusion is also presented in the study of Groß](#)
316 [and Müller \(2021\).](#)

317

318 Furthermore, we applied another loss estimation method to test robustness of the extreme ozone loss values; the passive method
319 that uses a passive tracer (i.e. no chemistry) simulation. We have used the well-known and widely used TOMCAT/SLIMCAT
320 model simulations for the tracer calculations (Chipperfield et al., 1999; Dhomse et al., 2019). The ozone loss computed with
321 the passive method shows the peak value of about 2.3–2.5 ppmv at about 450 K in the Arctic winter 2020 (Figure 5, second
322 panel from the left). This ozone loss is slightly higher than that of the Arctic winter 2011, about 0.2 ppmv. It is also observed
323 that the ozone loss in 2020 is higher than that of 2011 below 475 K, but the loss estimated in the 2011 winter exceeds about
324 0.3–0.5 ppmv above 475 K up to 700 K (e.g. Manney et al., 2020; [Wohltmann et al., 2020](#)). However, these ozone loss
325 estimates are lower than those estimated with the descent method, by about 0.5–0.7 ppmv depending on altitude. The analysis

326 with ozone and N₂O from the model indicates that modelled ozone is higher than (by about 1–1.5 ppmv) the measurements at
327 these altitudes, which could be due to the slower dynamical descent in the model.

328

329 It is clear that the ozone loss in 2020 is the largest among Arctic winters so far. Therefore, we also examined the evolution of
330 chlorine activation in terms of the amount of ClO in each Arctic winter, as the total chlorine is decreasing in the stratosphere
331 due to the effect of Montreal Protocol (e.g. Strahan et al., 2017; WMO, 2018; Dhomse et al., 2019) and we expect a
332 corresponding response in ozone loss in the polar winters. Stratospheric halogen levels (EESC) in the Arctic in 2020 are more
333 than 10% below the maximum levels in 2000 (Groß und Müller, 2021). Figure 6 shows the MLS ClO observations, [the
334 December-February and December-March potential PSC areas, and EESC](#) in each winter since 2005. The analyses show that
335 the chlorine activation was very severe and continuous for about four months in 2020. However, the highest ClO and [largest
336 APSC](#) values were observed in winter of 2016. Many cold winters showed ClO values around 1.8–2.0 ppbv as found in 2020,
337 but the sustained chlorine activation that was observed in 2020 was unique. Although the high ClO values in March were also
338 observed in 2011, the chlorine activation was not as severe as in 2020 in early winter (December–January). [The record-
339 breaking ice PSCs in the winter 2020 might have also contributed to the exceptional chlorine levels.](#) On the other hand, the
340 unprecedented chlorine activation observed in 2016 was more episodic, such as in mid-December, mid-January to early
341 February and late February. Therefore, the continuous and severe chlorine activation from December through March was the
342 key for the record-breaking ozone loss in 2020. Figure 6(b) and (c) further illustrate that the peak ClO profiles or the time
343 series of average ClO for the entire winter will not reveal the depth of chlorine activation. [We also looked at the changes in
344 EESC during the period \(2005-2020\) and there has been continuous decline in EESC during the period \(Fig. 6, top panel\). The
345 rate of change of EESC during the period is about 246.16 ppt per year \(e.g. WMO, 2018\); suggesting a consistent reduction in
346 stratospheric halogen loading in 2020 \(e.g. Groß and Müller, 2021\).](#)

347 **3.6 The Arctic ozone loss and the Antarctic ozone loss**

348 The peak ozone loss in the Antarctic happens at around 500 K and the loss is severe from 400 to 600 K for five months
349 continuously from August to November (Tilmes et al., 2006; Huck et al., 2005; Sonkaew et al., 2013; Kuttippurath et al.,
350 2015). In contrast, the cold Arctic winters are normally shorter and maximum ozone loss occurs at around 425–475 K for a
351 period of about two months, from mid-January to mid-March (e.g. Kuttippurath et al., 2010; Manney et al., 2004). The ozone
352 loss in the Arctic is limited to the altitudes below 500 K. The ozone loss in the Arctic winter 2020 was very high, and therefore,
353 we compare the Arctic ozone loss in 2020 with that in the Antarctic winters 2015 and 2019. The Antarctic winter 2015 was
354 one of the coldest and 2019 was one of the warmest, and therefore, the assessment would give an upper and lower bound of
355 ozone loss estimate for the Arctic winter 2020.

356

357 The peak ozone loss estimated using the vortex descent method is about 2.8 ppmv at 480 K in the Antarctic winter 2015 and
358 about 2.3 ppmv at 490 K in 2019 (Figure 5). The ozone loss in the Antarctic winter 2015 shows consistently higher values

359 (about 0.1–0.5ppmv) than that of 2019 up to 550 K, and the loss is similar above that altitude in both winters. The ozone loss
360 is about 1.0 ppmv at 370 K, 2.6 ppmv at 460 K, 1.5 ppmv at 550 K, 0.5 ppmv at 650 K and it terminates at 700 K in the
361 Antarctic winter 2015. In the Arctic winter 2020, the ozone loss shows about 0.3 ppmv at 370 K, 2.0 ppmv at 430 K and 480
362 K, 1.5 ppmv at 550 K and loss terminates above that altitude. The peak ozone loss is about 2.3 ppmv at 460–470 K. On the
363 other hand, the loss in the Antarctic winters above 470 K is very large and reaching up to 700 K. The peak ozone loss in the
364 Arctic winter 2020 is about 2.8 (2.3) ppmv and is at 460–470 K. This is also the main difference between the Arctic and
365 Antarctic ozone loss, as the broader and larger ozone loss occurs above the 470 K in the Antarctic. The difference is almost
366 1.0 ppmv above the peak ozone loss altitude. Therefore, the ozone loss in the Arctic winter 2020 is either equal or larger than
367 that of the Antarctic winter 2019 below 470 K, but the loss is smaller than that of the Antarctic winters above 525 K.
368

369 We have also applied the passive method to further examine the estimated loss in the Arctic and Antarctic winters (Figure 5,
370 second panel from the left). The ozone loss estimated with the passive method exhibits smaller values in the lower stratosphere
371 in comparison with that derived from the descent method. The loss is about 0.2 ppmv at 350 K, 1.6 ppmv at 400 K and 2.3
372 ppmv at 450 K in the Arctic winter 2020. The peak loss is recorded at 450–460 K and the loss decreases with altitude, about
373 1.5 ppmv at 500 K and 0.1 ppmv at 530 K. In the Antarctic winter 2019, the ozone loss shows similar values as that of the
374 Arctic winter 2020 at 370–420 K, but slightly smaller than that of the Arctic winter at 420–470 K. The maximum ozone loss
375 in Antarctic winter 2019 is estimated at 470 K, about 2.3 ppmv, and about 0.5–1.5 ppmv above that altitude, which is higher
376 than that of the Arctic winter 2020. Furthermore, the Arctic ozone loss halts at about 550 K, whereas the Antarctic ozone loss
377 at this altitude is as high as 1.5 ppmv. In the Antarctic winter 2015, the ozone loss is about 1.0 ppmv at 370 K, 2.0 ppmv at
378 400 K and the peak loss of about 2.8 ppmv at 475 K. The loss gradually decreases with altitude, such as 2.1 ppmv at 500 K,
379 1.5 ppmv at 550 K, 1.0 ppmv at 600 K and 0.5 ppmv at 650 K. The diagnosed ozone loss in the Antarctic winter 2015 is thus,
380 higher than that of the Antarctic winter 2019 and the Arctic winter 2020, by about 0.5–1.5 ppmv, depending on the altitude.
381 The assessment further gives strong evidence that the peak ozone loss in the Arctic winter 2020 is similar to that of the warm
382 winters of Antarctic (e.g. 2019). The loss estimation method can have uncertainty in the range of 3–5%, depending on the
383 winter months. For instance, the monthly mean ozone loss and its standard deviation for each winter month of 2020 are shown
384 in Figure S3. A complete error analyses of the passive method to estimate ozone loss is already presented in Kuttippurath et
385 al. (2010).

386 **3.7 The first appearance of ozone loss saturation in the Arctic**

387 Ozone loss saturation (i.e. O_3 values less than 0.1 ppmv) is a common feature of Antarctic winters since 1987 (Solomon et al.,
388 2005; Kuttippurath et al., 2018; Jin et al., 1996). However, as compared to the Antarctic, the Arctic winters are relatively short
389 (December–March), stratospheric temperatures are about 10 K higher, occurrence of PSCs are infrequent, denitrification is
390 modest and thus, ozone loss is generally more moderate. **Therefore, the Arctic never encountered the ozone loss saturation** (i.e.
391 the near complete (about 90–95%) loss of ozone at some altitudes in the lower stratosphere between 400 and 550 K) there

392 before. Apart from these, [the vortex-averaged ozone loss](#) normally happens [only up to 25–30% in the Arctic winters in](#)
393 [accordance with ground-based spectrometer observations and henceforth](#), a loss saturation was unexpected for Arctic
394 conditions. Figure 5 (right) shows the ozone profile measurements by ozonesondes at two Arctic stations, Alert (82.50° N,
395 62.33° W) and Eureka (80.05 N, 86.42 W), on selected days. The ozone profiles measured at selected Antarctic stations are
396 also shown for comparisons. In general, the ozone loss saturation in Antarctica occurs at the altitude between 400 and 500 K
397 (e.g. Davis: 68.6°S, 78.0°E and Marambio: 64° S, 56° W), and the altitude range would go up to 550 K for the stations that are
398 always inside the vortex, as shown for Syowa. [Note that the ozone loss saturation is taken as 0.2 ppmv and ozone detection](#)
399 [limit of sondes is 10 ppbv](#) (Kuttippurath et al., 2018; Solomon et al., 2005; Vömel and Diaz, 2010). The ozone loss observed
400 at Davis and Marambio is always smaller than that at Neumayer, South Pole and Syowa. Therefore, ozone loss saturation is
401 also different at different stations in the Antarctic. Here, the ozonesonde measurements at Alert (on [08 April 2020](#)) show loss
402 saturation at the altitudes 420–475 K (e.g. [Wilka et al., 2021](#)). The measurements at Eureka (on [10 April 2020](#)) show loss
403 saturation with about 99% ozone loss at altitudes between 420 and 460 K ([see also Bogner et al., 2021](#)). The time series of
404 ozone measurements, as analysed from the available measurements, show that the ozone loss saturation occurred at these
405 stations in early April (Figure S4). The vertical shading in Figure 5 for 0.2 ppmv shows the ozone loss saturation criterion with
406 respect to the ozone volume mixing ratios and the ozonesonde measurements have an uncertainty of [5–10%](#) (Smit et al., 2007).
407 Yet, the ozone measurements at Alert and Eureka are in the saturation limit and thus, provide first evidence for the occurrence
408 of ozone loss saturation in the Arctic. The loss saturation suggests that the Arctic polar stratospheric has [entered a new era of](#)
409 [change. Our analyses are consistent with the analyses of Wohltmann et al. \(2020\), who report about 90–93% loss of ozone in](#)
410 [the 450–475 K range in 2020](#) and with those of Groöß and Müller (2021) who find a lowest simulated ozone mixing ratio of
411 about 40 ppbv in 2020.

412 [3.8 Days with ozone values below a threshold of 220 DU](#)

413 Since the Antarctic ozone hole is defined with respect to TCO measurements (i.e. below 220 DU), we analysed TCO
414 measurements for the Arctic in 2020, which are shown in Figure 7. It shows the lowest TCO measurements made in the Arctic
415 polar region in the winter of 2020 by three different satellite instruments, OMI, OMPS and GOME. As shown (Fig. 7), the
416 OMI measurements show TCO below 300 DU for almost all winter months inside the vortex, as defined by [Nash et al. \(1996\)](#).
417 The measurements show around 230 DU in early December, about 260 DU in January, about 218–260 DU in February, around
418 220 DU in March and around 240 DU in April. There are ozone values lower than or equal to 220 DU in early (01–05)
419 December, late (25–26) January, some days (05, 12 and 17–22) in March and few days in early (06–07) April. The occurrences
420 of these low ozone values in December and January are associated with ozone mini-holes triggered by dynamics. However,
421 the appearances of extremely low TCO, below 220 DU, values in March and April are driven by chemistry and this is our topic
422 of discussion. The very low ozone measured by OMI corresponding to the dates are also shown in the ozone maps in the top
423 panel and the exact dates of extremely low ozone occurrences based on OMPS and MERRA-2 data are given in Table S1. The
424 OMPS total column agrees well with that of the OMI measurements throughout the period, where the differences are mostly

425 2–3 DU and are within the uncertainty of both instruments (i.e. about 5–10%). The OMPS measurements have captured all
426 features of OMI measurements throughout the winter. The GOME measurements are very close to the OMI and OMPS
427 measurements too, but are slightly higher in January and February due to the limited coverage of northern polar region by
428 GOME in winter months. As the winter progresses, the GOME coverage improves and therefore, the March and April
429 measurements are in excellent agreement with other satellite observations. The TCO measurements at Alert also manifest the
430 low ozone values of about 200 DU in two days of April; corroborating the satellite observations (Figure 7).

431

432 We also estimated the partial column ozone loss from the ozone profiles of OMPS and MLS satellites (Figure 7, bottom panel).
433 The ozone loss is calculated with respect to the passive method (Feng et al., 2005). The Arctic winters usually show total
434 column ozone (TCO) loss of about 70–80 DU in cold winters, about 45–50 DU in warm winters, and about 90–110 DU in
435 exceptionally cold winters such as in 2005 and 2011 (Goutail et al., 2005; Kuttippurath et al., 2012b; Rex et al., 2005; Manney
436 et al., 2003). The largest column ozone loss ever measured was in the Arctic winter 2011, and was about 110 DU as assessed
437 from all available studies (Griffin et al., 2018; Kuttippurath et al., 2012; Manney et al., 2011). On the other hand, the Antarctic
438 ozone column loss is about twice that of the Arctic, about 150–160 DU, but slightly lower about 100–120 DU in very warm
439 winters (1988 and 2002) and in early years (e.g. 1979–1985) of ozone loss there (Huck et al., 2005; Tilmes et al., 2006;
440 Kuttippurath et al., 2015). The analyses suggest that even the partial column ozone loss in the Arctic winter 2020 is about 115
441 DU at 350–550 K, which is higher than that of the Arctic winter 2011 and similar to that of the loss found in the Antarctic
442 winters 1979–1985, 2002 and 2019.

443

444 Since the ozone loss in the Arctic winter 2020 is up to the levels of that found in some Antarctic winters, we examined the
445 occurrence of extremely low TCO values using data from OMPS and MERRA-2; the results are presented in Figure 8 for
446 selected days. The first appearance of ozone holes in Antarctic winters is also shown for comparison. There are clear and
447 identifiable regions of extremely low TOC (regions below 220 DU) in March and April 2020, which were hundreds of
448 kilometres wide (see also Dameris et al., 2021). The ozone maps show that the low ozone regions in March and April 2020
449 were larger than those measured in the Antarctic in October 1979 and 1980. Therefore, ozone loss in the Arctic winter 2020 is
450 roughly comparable to the Antarctic ozone loss at about 1980. The appearance of a threshold in TCO below 220 DU for several
451 weeks demonstrates that Arctic winters may enter a new era of ozone depletion events, and signal significant changes in the
452 climate of the region (e.g. von der Gathen et al., 2021). However, extremely low TOC values neither appeared in all parts of
453 the vortex nor are present continuously for months as they occur over the Antarctic; further, very strong chemical ozone loss
454 occurs very regularly in the Antarctic, whereas strong Arctic ozone loss occurs only in very cold years (Bodeker et al., 2005;
455 Tilmes et al., 2006; Feng et al., 2007; Müller et al., 2008; von der Gathen et al., 2021).

456

457

458

459 **4. Conclusions**

460 The Antarctic ozone hole has been present for the past forty years, and the impact of ozone hole on public health is mostly
461 restricted to the southern high and mid-latitudes. The ozone hole has also influenced the climate of southern hemisphere by
462 changing the winds, temperature and precipitation in different regions. On the other hand, the biggest concern about the polar
463 ozone loss in the stratosphere has always been strong Arctic ozone loss, because such an ozone reduction can occur anywhere
464 beyond 45° N in the densely populated northern mid and high latitudes. The changes in associated UV radiation incidence
465 would also affect the flora and fauna of the region. If such a situation arose, it would trigger ecosystem damage and impose a
466 serious threat to public health (e.g. Newman et al., 2009). [An account of the record breaking increase in UV radiation in the](#)
467 [2019/20 Arctic winter is presented by Bernhard et al. \(2020\)](#). Nevertheless, it is believed that extreme reductions in column
468 ozone over the Arctic would be unlikely due to relatively higher temperature and a shorter wintertime ozone loss period there.
469 Furthermore, Arctic winters are always prone to several minor and frequent major warmings (almost a major warming per
470 winter), which would restrict the lifetime of the polar vortex, PSC occurrence and chlorine activation to limit the extent and
471 severity of ozone loss. However, the Arctic winter 2020 was exceptional as it was characterised by a strong vortex from
472 December through the end of April, large and widespread PSC occurrence, and unprecedented and prolonged chlorine
473 activation with peak ClO values of about 2.0 ppbv. The high chlorine activation in early December and early January produced
474 larger loss in ozone (e.g. 1–1.5 ppmv below 430 K in early January) in the Arctic that has never occurred before, consistent
475 with the results of the studies of [Weber et al. \(2021\)](#) and [Innes et al. \(2020\)](#). The continued high chlorine activation from
476 January to mid-April caused a record-breaking ozone loss of about 2.5–3.4 ppmv at 400–600 K, and triggered the first-ever
477 [observation of extremely low ozone columns in the Arctic in March and April 2020](#). The unprecedented chlorine activation
478 (e.g. January through March, above 0.7 ppbv) and severe denitrification (60–80%) also set up the atmosphere to have the first
479 ever occurrence of ozone loss saturation in the Arctic. Another interesting aspect of this winter was the dynamically driven
480 but chemically modified ozone mini-holes in December and January. These mini-holes were larger than the Antarctic ozone
481 holes of 1979 and early 1980s. [The analyses presented use multiple data sets, different ozone loss estimation methods, and](#)
482 [several parameters to make a robust statistics and a balanced assessment of the polar ozone depletion in the Arctic winter /spring](#)
483 [2020](#).

484 **Acknowledgements**

486 We thank Head CORAL, and the Director of Indian Institute of Technology Kharagpur (IIT KGP), Ministry of Human
487 Resource Development (MHRD), and Naval Research Board (OEP) of Defense Research and Development Organisation for
488 facilitating the study. PK and SR acknowledge the support from MHRD and IIT KGP. GSG and JK acknowledge the funding
489 from DRDO OEP. We thank the data managers and the scientists who worked hard for making available the MLS, OMPS,
490 OMI, MERRA, ER5, ozonesonde, GOME, and all other data for this study. We also thank the HYSPLIT model developers
491 for the trajectory analyses. The authors thank Paul Newman, Larry Flynn, Lucien Froidevaux, Jonathan Davies, Peter von der

492 Gathen and Martyn Chipperfield for their help and support in making this article happen. The SLIMCAT forced by ERA5
493 simulation was performed on the University of Leeds ARC4HPC system.

494

495 **Data availability**

496 The MLS data are available on <https://disc.gsfc.nasa.gov/>. The MODIS datasets were acquired from the Level-1 and
497 Atmosphere Archive & Distribution System (LAADS) Distributed Active Archive Center (DAAC), located in the Goddard
498 Space Flight Center in Greenbelt, Maryland (<https://ladsweb.nascom.nasa.gov/>). The ozonesonde data are available from the
499 World Ozone and Ultraviolet Radiation Data Centre (WOUDC, <https://woudc.org/>). The OMPS ozone data are available on
500 <https://earthdata.nasa.gov/earth-observation-data/near-real-time/download-nrt-data/omps-nrt>. The meteorological analyses:
501 temperature, winds, heat flux, PSC and wave heat flux data are taken from <https://ozonewatch.gsfc.nasa.gov/>. The OMI data
502 are available on <https://disc.gsfc.nasa.gov/datasets/>. The GOME data are downloaded from the
503 <https://atmosphere.copernicus.eu/data>.

504

505 **Author Contributions**

506 JK conceived the idea and wrote the original manuscript. The manuscript was subsequently revised with inputs from RM and
507 WF. JK, PK, SR, RR and GK analysed the data and produced the figures. WF designed the model runs and carried out the
508 model simulations. All authors participated in the discussions and made suggestions, which were considered for the final draft.

509

510 **Additional information**

511 Supplementary Information accompanies the paper on this journal website.

512

513 **Competing Interests**

514 J. K. and R.M. are editors of ACP; otherwise, the authors declare no competing and conflict of interests

515 **References**

516 Bai, K., Liu, C., Shi, R. and Gao, W.: Comparison of Suomi-NPP OMPS total column ozone with Brewer and Dobson
517 spectrophotometers measurements, *Front. Earth Sci.*, 9, 369–380. <https://doi.org/10.1007/s11707-014-0480-5>, 2015.

518 Bai, K., Chang, N.-B., Yu, H. and Gao, W.: Statistical bias correction for creating coherent total ozone record from OMI and
519 OMPS observations, *Remote Sensing of Environment*, 182, 150–168, 2016.

520 Bais, A., et al.: Environmental effects of ozone depletion, UV radiation, and interactions with climate change: UNEP
521 Environmental Effects Assessment Panel, update 2019, *Photochem. Photobiol. Sci.*, 19, 542–584, 2020.

522 [Bernhard, G. H., et al.: Record-breaking increases in Arctic solar ultraviolet radiation caused by exceptionally large ozone
523 depletion in 2020. *Geophysical Research Letters*, 47, e2020GL090844. <https://doi.org/10.1029/2020GL090844> ,2020](#)

524 Bodeker G. E, Shiona H and Eskes H.: Indicators of Antarctic ozone depletion, *Atmos. Chem. Phys.*, 5, 2603–2615, 2005.

525 [Bognar, K., et al.: Unprecedented spring 2020 ozone depletion in the context of 20 years of measurements at Eureka, Canada.](#)

526 [Journal of Geophysical Research: Atmospheres](#), 126, e2020JD034365. <https://doi.org/10.1029/2020JD034365>, 2021

527 [Bojkov, R. D. and Balis, D. S.: Characteristics of episodes with extremely low ozone values in the northern middle latitudes](#)

528 [1957–2000, *Ann. Geophys.*, 19, 797–807, <https://doi.org/10.5194/angeo-19-797-2001>, 2001.](#)

529 Brasseur, G. and Solomon, S.: *Aeronomy of the Middle Atmosphere*. D. Reidel Publishing Company, Dordrecht, ISBN 90-

530 277-1767-2 (Netherlands), 1984.

531 Bremer, H. et al.: Ozone depletion observed by the Airborne Submillimeter Radiometer (ASUR) during the Arctic winter

532 1999/2000, *J. Geophysical Research*, 107, 1–7, 2002.

533 [Canziani, P. O., Compagnucci, R. H., Bischoff, S. A., and Legnani, W. E.: A study of impacts of tropospheric synoptic](#)

534 [processes on the genesis and evolution of extreme total ozone anomalies over southern South America, *J. Geophys. Res. -*](#)

535 [Atmos.](#), 107, 4741, <https://doi.org/10.1029/2001JD000965>, 2002.

536 Chipperfield, M. P.: New version of the TOMCAT/SLIMCAT off-Line chemical transport model: Intercomparison of

537 stratospheric tracer experiments, *Q. J. R. Meteorol. Soc.*, 132, 1179–1203, doi:10.1256/qj.05.51, 2006.

538 Chipperfield, M. P., et al.: Detecting Recovery of the Stratospheric Ozone Layer, *Nature*, 549, 211–218,

539 doi:10.1038/nature23681, 2017.

540 Chubachi, S.: Preliminary result of ozone observations at Syowa from February 1982 to January 1983, *Mem. Natl Inst. Polar*

541 *Res.*, Special Issue, 34, 13–19, 1984.

542 Coy, L., Nash, E. R. and Newman, P. A.: Meteorology of the polar vortex: Spring 1997, *Geophys. Res. Lett.*, 24, 2693–2696,

543 1997.

544 [Dameris, M., Loyola, D. G., Nützel, M., Coldewey-Egbers, M., Lerot, C., Romahn, F., and van Roozendaal, M.: Record low](#)

545 [ozone values over the Arctic in boreal spring 2020, *Atmos. Chem. Phys.*, 21, 617–633, \[https://doi.org/10.5194/acp-21-617-\]\(https://doi.org/10.5194/acp-21-617-2021\)](#)

546 [2021](#), 2021.

547 [DeLand, M. T., Bhartia, P. K., Kramarova, N., and Chen, Z.: OMPS LP observations of PSC variability during the NH 2019–](#)

548 [2020 season. *Geophysical Research Letters*, 47, e2020GL090216. <https://doi.org/10.1029/2020GL090216>, 2020](#)

549 Drdla, K. and Müller, R.: Temperature thresholds for chlorine activation and ozone loss in the polar stratosphere, *Ann.*

550 *Geophys.*, 30, 1055–1073, <https://doi.org/10.5194/angeo-30-1055-2012>, 2012.

551 Dhomse, S. S., Feng, W., Montzka, S. A. et al.: Delay in recovery of the Antarctic ozone hole from unexpected CFC-11

552 emissions, *Nat Commun.*, 10, 5781. <https://doi.org/10.1038/s41467-019-13717-x>, 2019.

553 [Dobson, G. M. B., Harrison, D. N.: Measurements of the amount of ozone in the Earth's atmosphere and its relation to other](#)

554 [geophysical conditions: part I. *Proceedings of the Royal Society of London, Series A* 110: 660–693, 1926](#)

555 Engel, A., Bönisch, H., Ostermüller, J., Chipperfield, M. P., Dhomse, S., and Jöckel, P.: A refined method for calculating

556 equivalent effective stratospheric chlorine, *Atmos. Chem. Phys.*, 18, 601–619, <https://doi.org/10.5194/acp-18-601-2018>, 2018.

557 Farman, J. C., Gardiner, B. G. and Shanklin, J. D.: Large losses of total ozone in Antarctica reveal seasonal ClO x/NOx
558 interaction, *Nature*, 315, 207–210, 1985.

559 Feng, W., Chipperfield, M. P., Davies, S., von der Gathen, P., Kyrö, E., Volk, C. M., Ulanovsky, A. and Belyaev, G.: Large
560 chemical ozone loss in 2004/2005 Arctic winter/spring, *Geophys. Res. Lett.*, 34, L09803, doi:10.1029/2006GL029098, 2007.

561 Feng, W. et al.: Three-Dimensional Model Study of the Antarctic Ozone Hole in 2002 and Comparison with 2000,
562 <http://dx.doi.org/10.1175/JAS-3335.1> 62, 822–837, 2005.

563 Feng, W., Fast Ozone Loss Around the Polar Vortex During 2002/2003 Arctic Winter Deep Minihole Event, *Water, Air, and*
564 *Soil Pollution*, Vol.171: 383-397, 2006.

565 Feng, W., Chipperfield, M. P., Davies, S., Mann, G. W., Carslaw, K. S., Dhomse, S., Harvey, L., Randall, C., and Santee, M.
566 L.: Modelling the effect of denitrification on polar ozone depletion for Arctic winter 2004/2005, *Atmos. Chem. Phys.*, 11,
567 6559–6573, <https://doi.org/10.5194/acp-11-6559-2011>, 2011.

568 Feng, W., Dhomse, S. S., Arosio, C., Weber, M., Burrows, J. P., Santee, M. L., and Chipperfield, M. P.: Arctic ozone depletion
569 in 2019/20: Roles of chemistry, dynamics and the Montreal Protocol. *Geophysical Research Letters*, 48, e2020GL091911.
570 <https://doi.org/10.1029/2020GL091911>, 2021

571 Flynn, L., et al.: Performance of the Ozone Mapping and Profiler Suite (OMPS) products, *J. Geophys. Res. Atmos.*, 119, 6181–
572 6195, doi:10.1002/2013JD020467, 2014.

573 Gelaro, R. et al.: The Modern-Era Retrospective Analysis for Research and Applications, Version 2 (MERRA -2), *J. Climate*,
574 30, 5419–5454, <https://doi.org/10.1175/JCLI-D-16-0758.1>, 2017.

575 Goutail, F. et al.: Early unusual ozone loss during the Arctic winter 2002/2003 compared to other winters, *Atmos. Chem*
576 *Phys.*, 5, 665–677, doi:10.5194/acp-5-665-2005, 2005.

577 Griffin, D. et al.: Stratospheric ozone loss in the Arctic winters between 2005 and 2013 derived with ACE-FTS measurements,
578 *Atmospheric Chemistry and Physics*, 19, 577–601, 2019.

579 Griffin, D., Walker, K. A., Wohltmann, I., Dhomse, S. S., Rex, M., Chipperfield, M. P., Feng, W., Manney, G. L., Liu, J. and
580 Tarasick, D.: Stratospheric ozone loss in the Arctic winters between 2005 and 2013 derived with ACE-FTS measurements,
581 *Atmos. Chem. Phys.*, 19, 577–601, <https://doi.org/10.5194/acp-19-577-2019>, 2019.

582 Groß, J.-U., and Müller, R.: Simulation of record Arctic stratospheric ozone depletion in 2020. *Journal of Geophysical*
583 *Research: Atmospheres*, 126, e2020JD033339. <https://doi.org/10.1029/2020JD033339>, 2021

584 Huck, P. E., McDonald, A. J., Bodeker, G. E. and Struthers, H.: Interannual variability in Antarctic ozone depletion controlled
585 by planetary waves and polar temperature, *Geophysical Research Letters*, 32, doi:10.1029/2005GL022943, 2005.

586 Hurwitz, M. M., Newman, P. A., and Garfinkel, C. I.: The Arctic vortex in March 2011: a dynamical perspective, *Atmos.*
587 *Chem. Phys.*, 11, 11447–11453, doi:10.5194/acp-11-11447-2011, 2011.

588 Inness, A., et al.: Exceptionally low Arctic stratospheric ozone in spring 2020 as seen in the CAMS reanalysis. *Journal of*
589 *Geophysical Research: Atmospheres*, 125, e2020JD033563. <https://doi.org/10.1029/2020JD033563>, 2020

590 IPCC. 2007. B. Metz, O.R. Davidson, P.R. Bosch, R. Dave, L.A. Meyer (eds.): Contribution of Working Group III to the
591 Fourth Assessment Report of the Intergovernmental Panel on Climate Change, Cambridge University Press, Cambridge,
592 United Kingdom and New York, NY, USA, 2007.

593 James PM.: A climatology of ozone mini-holes over the Northern Hemisphere. *International Journal of Climatology* 18: 1287–
594 1303, 1998.

595 James PM, Peters D, Greisinger KM.: A study of ozone mini-hole formation using a tracer advection model driven by
596 barotropic dynamics. *Meteorology and Atmospheric Physics* 64: 107–121, 1997.

597 Jiang, Y., Yung, Y. L. and Zurek, R. W.: Decadal evolution of the Antarctic ozone hole, *J. Geophys. Res.*, 101, 8985–8999,
598 1996.

599 Jin, J. J. et al.: Severe Arctic ozone loss in the winter 2004/2005: observations from ACE-FTS. *Geophysical Research Letters*,
600 33, L15801, 2006.

601 Kirner, O., Müller, R., Ruhnke, R., and Fischer, H.: Contribution of liquid, NAT and ice particles to chlorine activation and
602 ozone depletion in Antarctic winter and spring, *Atmos. Chem. Phys.*, 15, 2019–2030, [https://doi.org/10.5194/acp-15-2019-](https://doi.org/10.5194/acp-15-2019-2015)
603 [2015](https://doi.org/10.5194/acp-15-2019-2015), 2015.

604 Kivi, R. et al.: Ozone sonde observations in the Arctic during 1989–2003: Ozone variability and trends in the lower stratosphere
605 and free troposphere, *J. Geophys. Res.*, 112, D08306, doi:10.1029/2006JD007271, 2007.

606 Kramarova et al.: Measuring the Antarctic ozone hole with the new Ozone Mapping and Profiler Suite (OMPS), *Atmos. Chem*
607 *Phys.*, 14, 2353–2361, <https://doi.org/10.5194/acp-14-2353-2014>, 2014.

608 Kroon, M et al.: Comparing OMI-TOMS and OMI-DOAS total ozone column data, *J. Geophys. Res.*, 113, D16S28,
609 doi:10.1029/2007JD008798, 2008.

610 Krzysycin, J. W.: Long-term changes in ozone mini-hole event frequency over the Northern Hemisphere derived from ground-
611 based measurements. *International Journal of Climatology*, 22(12), 1425–1439. doi:10.1002/joc.812, 2002.

612 Kuttippurath, J. et al.: Spatial, temporal, and vertical variability of polar stratospheric ozone loss in the Arctic winters 2004/05–
613 2009/10, *Atmos. Chem. Phys.*, 10, 9915–9930, doi:10.5194/acp-10-9915-2010, 2010.

614 Kuttippurath, J., A. Kleinboehl, M. Sinnhuber, H. Bremer, H. Kuellmann, J. Notholt, S. Godin-Beekmann, O. P. Tripathi, and
615 G. Nikulin: Arctic ozone depletion in 2002—2003 measured by ASUR and comparison with POAM observations, *J. Geophys.*
616 *Res.*, doi:10.1029/2011JD016020 (Impact factor 3.826), 2011.

617 Kuttippurath, J. et al.: Record-breaking ozone loss in the Arctic winter 2010/2011: comparison with 1996/1997, *Atmospheric*
618 *Chemistry and Physics*, 2012, 7073–7085, doi:10.5194/acp-12-7073-2012, 2012.

619 Kuttippurath, J., Lefevre, F., Pommereau, J.-P., Roscoe, H. K., Goutail, F., Pazmino, A. & Shanklin, J. D.: Antarctic ozone
620 loss in 1979–2010: first sign of ozone recovery, *Atmos. Chem. Phys.*, 13, 1625–1635, doi:10.5194/acp-13-1625-2013, 2013.

621 Kuttippurath, J., Godin-Beekmann, S., Lefèvre, F., Santee, M.L., Froidevaux, L., Hauchecorne, A.: Variability in Antarctic
622 ozone loss in the last decade (2004–2013): high-resolution simulations compared to Aura MLS observations, *Atmos. Chem.*
623 *Phys.*, 15, 10385–10397, 2015.

624 Kuttippurath, J. et al.: Emergence of ozone recovery evidenced by reduction in the occurrence of Antarctic ozone loss
625 saturation. *npj Clim. Atmos. Sci.*, 1, 42. <https://doi.org/10.1038/s41612-018-0052-6>, 2018.

626 de Laat, A. and van Weele, M.: The 2010 Antarctic ozone hole: Observed reduction in ozone destruction by minor sudden
627 stratospheric warmings, *Sci. Rep.*, 1, 38. <https://doi.org/10.1038/srep00038>, 2011.

628 Lawrence, Z. D., et al.: The remarkably strong Arctic stratospheric polar vortex of winter 2020: Links to record-breaking
629 Arctic Oscillation and ozone loss. *Journal of Geophysical Research: Atmospheres*, 125, e2020JD033271.
630 <https://doi.org/10.1029/2020JD033271,2020>

631 Livesey, N. J., Santee, M. L., and Manney, G. L.: A Match-based approach to the estimation of polar stratospheric ozone loss
632 using Aura Microwave Limb Sounder observations, *Atmos. Chem. Phys.*, 15, 9945–9963, [https://doi.org/10.5194/acp-15-](https://doi.org/10.5194/acp-15-9945-2015)
633 9945-2015, 2015.

634 Lindenmaier, R. et al.: Unusually low ozone, HCl, and HNO₃ column measurements at Eureka, Canada during winter/spring
635 2011, *Atmos. Chem. Phys.*, 12, 3821–3835, doi:10.5194/acp-12-3821-2012, 2012.

636 Lefevre F. et al.: The 1997 Arctic ozone depletion quantified from three-dimensional model simulations, *Geophys. Res. Lett.*,
637 25, 2425–2428, 1998.

638 Layola, D. G. et al.: The GOME-2 total column ozone product: Retrieval algorithm and ground-based validation, *J. Geophys.*
639 *Res.*, 116, D07302, doi:10.1029/2010JD014675, 2011.

640 Manney G. L. et al. 2011. Unprecedented Arctic ozone loss in 2011, *Nature*, 478, 469–475, doi:10.1038/nature10556, 2011.

641 Manney, G. L., Livesey, N. J., Santee, M. L., Froidevaux, L., Lambert, A., and Lawrence, Z. D., et al.: Record-low Arctic
642 stratospheric ozone in 2020: MLS observations of chemical processes and comparisons with previous extreme winters,
643 *Geophysical Research Letters*, 47. <https://doi.org/10.1029/2020GL089063>, 2020

644 Manney, G. L., et al.: Variability of ozone loss during Arctic winter (1991–2000) estimated from UARS Microwave Limb
645 Sounder measurements, *J. Geophys. Res.*, 108(D4), 4149, doi:10.1029/2002JD002634, 2003.

646 McKenna, D., Jones, R. L., Austin, J., Browell, E. V., McCormick, M. P., Krueger, A. J., and Tuck, A. F.: Diagnostic studies
647 of the Antarctic vortex during the 1987 Airborne Antarctic Ozone Experiment: Ozone mini-holes, *J. Geophys. Res.*, 94, 11
648 641–11 668, 1989.

649 Millán, L. F., & Manney, G. L.: An assessment of ozone mini-hole representation in reanalyses over the Northern Hemisphere.
650 *Atmospheric Chemistry and Physics*, 17(15), 9277–9289. doi:10.5194/acp-17-9277-2017, 2017.

651 Müller, R., Groöß, J.-U., Lemmen, C., Heinze, D., Dameris, M., and Bodeker, G.: Simple measures of ozone depletion in the
652 polar stratosphere, *Atmos. Chem. Phys.*, 8, 251–264, <https://doi.org/10.5194/acp-8-251-2008>, 2008.

653 McPeters, R. D., S. Frith, and G. J. Labow.: OMI Total Column Ozone: Extending the Long-Term Data Record, *Atmospheric*
654 *Measurement Techniques*, 8, 4845–4850. doi:10.5194/amt-8-4845-2015, 2015.

655 Nair, P. J. et al. 2015. Subtropical and mid-latitude ozone trends: implications for recovery, *J. Geophys. Res.*, 7247–7257.

656 Nash, E. R., Newman, P. A., Rosenfield, J. E. and Schoeberl, M. R.: An objective determination of the polar vortex using
657 Ertel’s potential vorticity, *J. Geophys. Res.*, 101, 9471–9478, 1996.

658 Newman, P., E. Nash, and J. Rosenfeld.: What controls the temperature of the Arctic stratosphere during the spring? *J.*
659 *Geophys. Res.*, 106, 19999–20010, 2001.

660 Newman, P. A., Daniel, J. S., Waugh, D. W. and Nash, E. R.: A new formulation of equivalent effective stratospheric chlorine
661 (EESC), *Atmos. Chem. Phys.*, 7, 4537–4552, <https://doi.org/10.5194/acp-7-4537-2007>, 2007.

662 Newman, P. A., Lait, L. R. and Schoeberl, M. R.: The morphology and meteorology of southern hemisphere spring total ozone
663 mini-holes, *Geophys. Res. Lett.*, 15, 923–926, 1988.

664 Peters, D., Egger, J., and Entzian, G.: Dynamical aspects of ozone mini-hole formation. *Meteorology and Atmospheric*
665 *Physics*, 55(3–4), 205–214. doi:10.1007/bf01029827, 1995.

666 Pitts, M. C., Poole, L. R., and Thomason, L. W.: CALIPSO polar stratospheric cloud observations: second-generation detection
667 algorithm and composition discrimination, *Atmos. Chem. Phys.*, 9, 7577–7589, 2009.

668 Pommereau, J.-P. et al.: Recent Arctic ozone depletion: Is there an impact of climate change?, *C. R. Geosci.*, 350, 347–353,
669 2018.

670 Reed, R. J.: The role of vertical motions in ozone weather relationships, *J. Meteorol.*, 7, 263–267, <https://doi.org/10.1175/1520->
671 [0469\(1950\)007<0263:TROVMI>2.0.CO;2](https://doi.org/10.1175/1520-0469(1950)007<0263:TROVMI>2.0.CO;2), 1950.

672 Rex, M. et al. Arctic ozone loss and climate change, *Geophys. Res. Lett.*, 31, L04116, doi:10.1029/2003GL018844, 2004.

673 Rex, M. et al.: Chemical depletion of Arctic ozone in winter 1999/2000. *J. Geophysical Research* 107, 8276, 2002.

674 Rieder, H. E., and Polvani, L. M.: Are recent Arctic ozone losses caused by increasing greenhouse gases? *Geophys. Res. Lett.*,
675 40, 4437–4441, doi:10.1002/grl.50835, 2013.

676 Riese, M., Ploeger, F., Rap, A., Vogel, B., Konopka, P., Dameris, M., and Forster, P.: Impact of uncertainties in atmospheric
677 mixing on simulated UTLS composition and related radiative effects. *J. Geophys. Res.*, 117, D16305,
678 doi:10.1029/2012JD017751, 2012.

679 Rao, J., and Garfinkel, C. I.: Arctic ozone loss in March 2020 and its seasonal prediction in CFSv2: A comparative study with
680 the 1997 and 2011 cases. *Journal of Geophysical Research: Atmospheres*, 125, e2020JD033524.
681 <https://doi.org/10.1029/2020JD033524>, 2020

682 Salby, M., Titova, E. and Deschamps, L.: Rebound of Antarctic ozone, *Geophys. Res. Lett.*, 38, L09702,
683 doi:10.1029/2011GL047266, 2011.

684 Santee, M. L., Manney, G. L., Froidevaux, L., Zurek, R. W., and Waters, J. W.: MLS observations of ClO and HNO₃ in the
685 1996–97 Arctic polar vortex, *Geophys. Res. Lett.*, 24, 2713–2716, 1997.

686 Shaw, T. A. and Voigt, A.: Tug of war on summertime circulation between radiative forcing and sea surface warming, *Nature*
687 *Geoscience*, 8, 560–566, 2015.

688 Sinnhuber, B.-M. et al.: Arctic winter 2010/2011 at the brink of an ozone hole, *Geophys. Res. Lett.*, 38, L24814,
689 doi:10.1029/2011GL049784, 2011.

690 Sinnhuber, B.-M. et al.: Large loss of total ozone during the Arctic winters of 1999/2000, *Geophys. Res. Lett.*, 27, 3473–
691 3476, 2000.

692 Sofieva, V. F. et al.: Ozone CCI and OMPS ozone profile dataset and evaluation of ozone trends in the stratosphere,
693 Atmospheric Chemistry and Physics, 17, 12533–12552, 2017.

694 Solomon, S., Ivy, D. J., Kinnison, D., Mills, M. J., Neely, R. R., Schmidt, A.: Emergence of healing in the Antarctic ozone
695 layer, Science, 353, 269–274, 2016.

696 [Solomon, S., Portmann, R. W., Sasaki, T., Hofmann, D. J. & Thompson, D. W. J. Four decades of ozonesonde measurements
697 over Antarctica. J. Geophys. Res. 110, D21311, 2005.](#)

698 Sonkaew, T., von Savigny, C., Eichmann, K.-U., Weber, M., Rozanov, A., Bovensmann, H., Burrows, J. P., and
699 Groöß, J. U.: Chemical ozone losses in Arctic and Antarctic polar winter/spring season derived from SCIAMACHY
700 limb measurements 2002–2009, Atmos. Chem. Phys., 13, 1809–1835, doi:10.5194/acp-13-1809-2013, 2013.

701 Smit, H. G. et al.: Assessment of the performance of ECC ozonesondes under quasi flight conditions in the environmental
702 simulation chamber: insights from the Juelich Ozone Sonde Intercomparison Experiment (JOSIE), J. Geophys. Res., 112,
703 D19306, 2007.

704 Spang, R., Hoffmann, L., Müller, R., Groöß, J.-U., Tritscher, I., Höpfner, M., Pitts, M., Orr, A., and Riese, M.: A climatology
705 of polar stratospheric cloud composition between 2002 and 2012 based on MIPAS/Envisat observations, Atmos. Chem. Phys.,
706 18, 5089–5113, <https://doi.org/10.5194/acp-18-5089-2018>, <https://www.atmos-chem-phys.net/18/5089/2018/>, 2018.

707 Strahan, S. E. and A. R. Douglass, A. R.: Decline in Antarctic Ozone Depletion and Lower Stratospheric Chlorine Determined
708 from Aura Microwave Limb Sounder Observations, Geophysical Research Letters, 45, 382–390. doi:10.1002/2017GL074830,
709 2018.

710 [Stenke, A., and V. Grewe: Impact of ozone mini-holes on the heterogeneous destruction of stratospheric ozone, Chemosphere,
711 50, 177-190, \[https://doi.org/10.1016/S0045-6535\\(02\\)00599-4\]\(https://doi.org/10.1016/S0045-6535\(02\)00599-4\), 2003.](#)

712 Steinbrecht, W., Hassler, B., Claude, H., Winkler, P. and Stolarski, R. S.: Global distribution of total ozone and lower
713 stratospheric temperature variations, Atmos. Chem. Phys., 3, 1421–1438 doi:10.5194/acp-3-1421–2003, 2003.

714 Tilmes, S., Müller, R., Engel, A., Rex, M., and Russell III, J.: Chemical ozone loss in the Arctic and Antarctic
715 stratosphere between 1992 and 2005, Geophys. Res. Lett., 33, L20812, doi:10.1029/2006GL026925, 2006.

716 Tilmes, S., Müller, R., Salawitch, R. J., Schmidt, U., Webster, C. R., Oelhaf, H., Camy-Peyret, C. C. and Russell III, J. M.:
717 Chemical ozone loss in the Arctic winter 1991–1992, Atmos. Chem. Phys., 8, 1897–1910, [https://doi.org/10.5194/acp-8-1897-](https://doi.org/10.5194/acp-8-1897-2008)
718 [2008](#), 2008.

719 Thompson, D. W. J. and Solomon, S.: Interpretation of recent Southern Hemisphere climate change, Science, 296, 895–899,
720 2002.

721 Verhoelst, T. et al.: Metrology of ground-based satellite validation: co-location mismatch and smoothing issues of total ozone
722 comparisons, Atmospheric Measurement Techniques, 8, 5039–5062, 2015.

723 von der Gathen et al., Nature Comm., 2021.

724 Wargan, K., Kramarova, N., Weir, B., Pawson, S. and Davis, S. M.: Toward a Reanalysis of Stratospheric Ozone for Trend
725 Studies: Assimilation of the Aura Microwave Limb Sounder and Ozone Mapping and Profiler Suite Limb Profiler Data, Journal
726 of Geophysical Research, 125, 1–21, 2020.

727 Weber, M., et al.: Total Ozone Trends from 1979 to 2016 Derived from Five Merged Observational Datasets – The Emergence
728 into Ozone Recovery, Atmospheric Chemistry and Physics, 18, 2097–2117, doi:10.5194/acp-18-2097-2018, 2018.

729 Weber, M., et al.: The unusual stratospheric Arctic winter 2019/20: Chemical ozone loss from satellite observations and
730 TOMCAT chemical transport model. Journal of Geophysical Research: Atmospheres, 126, e2020JD034386.
731 <https://doi.org/10.1029/2020JD034386>, 2021

732 Wegner, T., Pitts, M. C., Poole, L. R., Tritscher, I., GroöB, J.-U., and Nakajima, H.: Vortex-wide chlorine activation by a
733 mesoscale PSC event in the Arctic winter of 2009/10, Atmos. Chem. Phys., 16, 4569–4577, [https://doi.org/10.5194/acp-16-](https://doi.org/10.5194/acp-16-4569-2016)
734 [4569-2016](https://doi.org/10.5194/acp-16-4569-2016), 2016.

735 Wilka, C., Solomon, S., Kinnison, D., and Tarasick, D.: An Arctic Ozone Hole in 2020 If Not For the Montreal Protocol,
736 Atmos. Chem. Phys. Discuss. [preprint], <https://doi.org/10.5194/acp-2020-1297>, in review, 2021.

737 Wohltmann, I., Lehmann, R., Rex, M., Brunner, D. and Maeder, J. A.: A process-oriented regression model for column ozone.
738 J. Geophys. Res. 112, D12304, doi:10.1029/2006JD007573, 2007.

739 Wohltmann, I., von der Gathen, P., Lehmann, R. et al.: Near-complete local reduction of Arctic stratospheric ozone by severe
740 chemical loss in spring 2020, Geophysical Research Letters, 47, <https://doi.org/10.1029/2020GL089547>, 2020.

741 World Meteorological Organization: Scientific Assessment of Ozone Depletion: 2010 (Report 52, Global Ozone Research and
742 Monitoring Project, 2011), 2010.

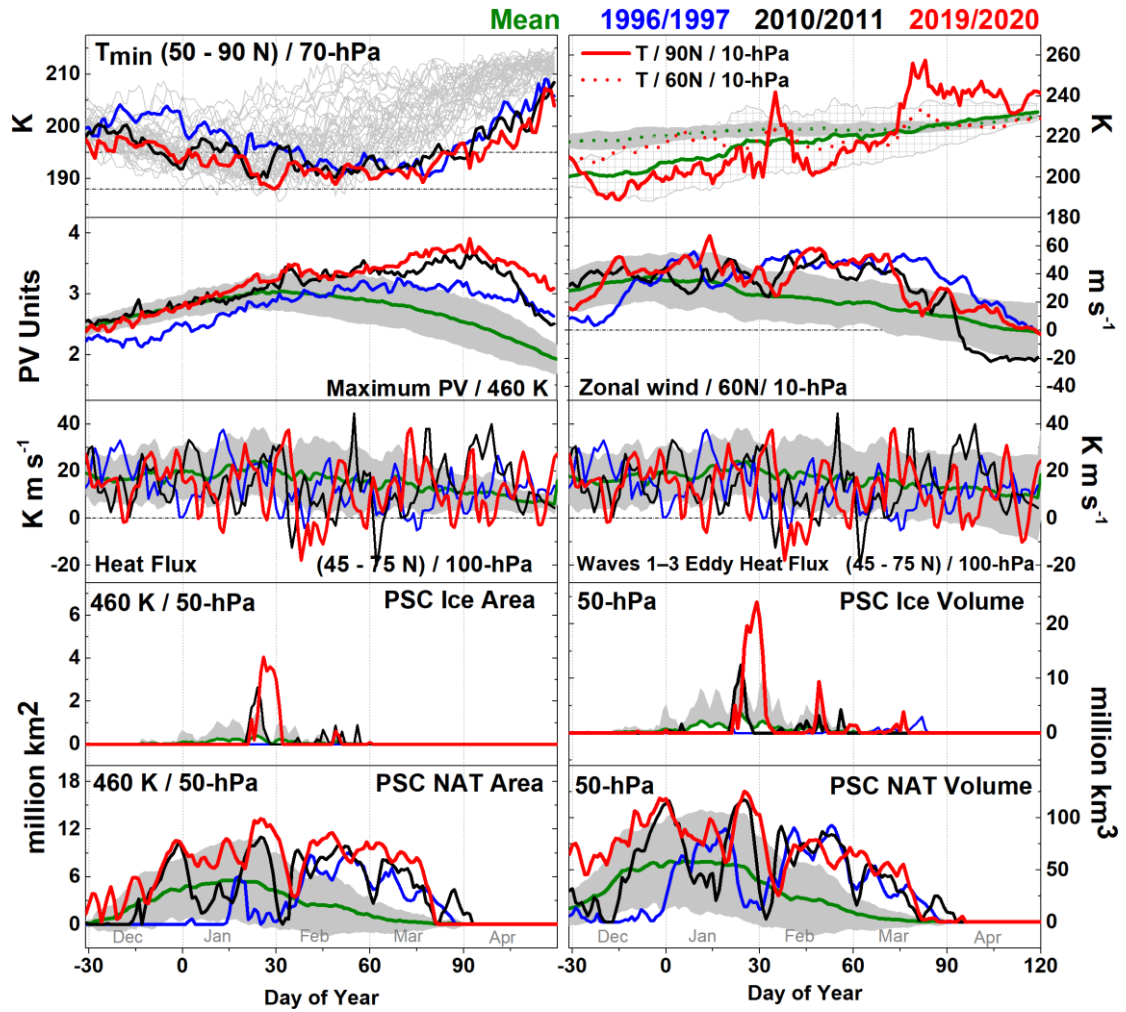
743 World Meteorological Organization. Scientific Assessment of Ozone Depletion: 2006 (Report 50, Global Ozone Research and
744 Monitoring Project, 2007), 2007.

745 Yamazaki, Y. et al.: September 2019 Antarctic sudden stratospheric warming: Quasi-6-day wave burst and ionospheric effects,
746 Geophysical Research Letters, 47, <https://doi.org/10.1029/2019GL086577>, 2020.

747 Yang, E.-S., Cunnold, D. M., Newchurch, M. J. & Salawitch, R. J.: Change in ozone trends at southern high latitudes, Geophys.
748 Res. Lett., 32, L12812, 2005.

749 Zhang, J. et al.: Stratospheric ozone loss over the Eurasian continent induced by the polar vortex shift, Nature Communications,
750 9, 206, 2018.

751
752
753
754



755

756 **Figure 1: Meteorology of the Arctic winter/spring 2020.** The temperature, zonal winds, potential vorticity (PV), heat flux,

757 wave eddy heat flux, and area and volume of polar stratospheric clouds (PSCs) for the Arctic winter 2020 as compared to

758 previous Arctic winters. The shaded area shows the standard deviation from the mean.

759

760

761

762

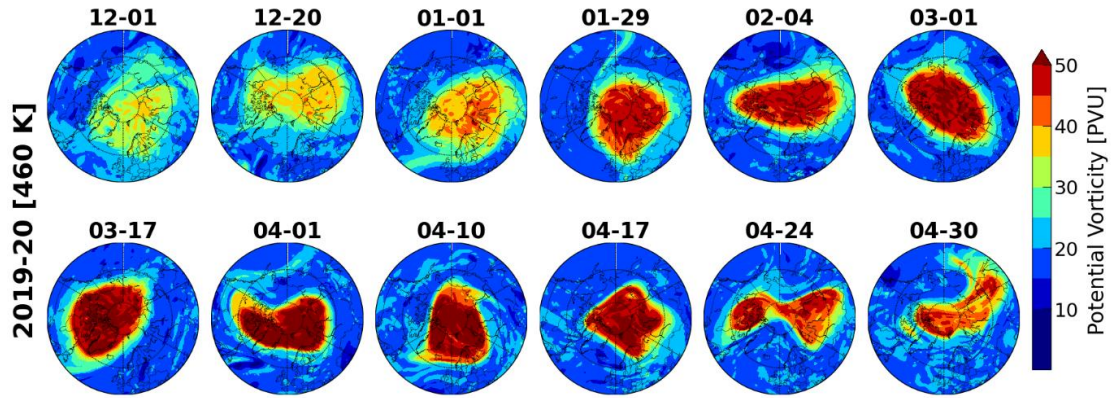
763

764

765

766

767



768

769 **Figure 2: Polar vortex evolution in the Arctic winter/spring 2020.** The evolution of polar vortex in the Arctic winter 2020.
770 The vortex situation in the lower stratospheric altitude of about 460 K (~17 km) is illustrated. The vortex edge is calculated
771 with respect to the Nash et al. (1996) criterion at each altitude.

772

773

774

775

776

777

778

779

780

781

782

783

784

785

786

787

788

789

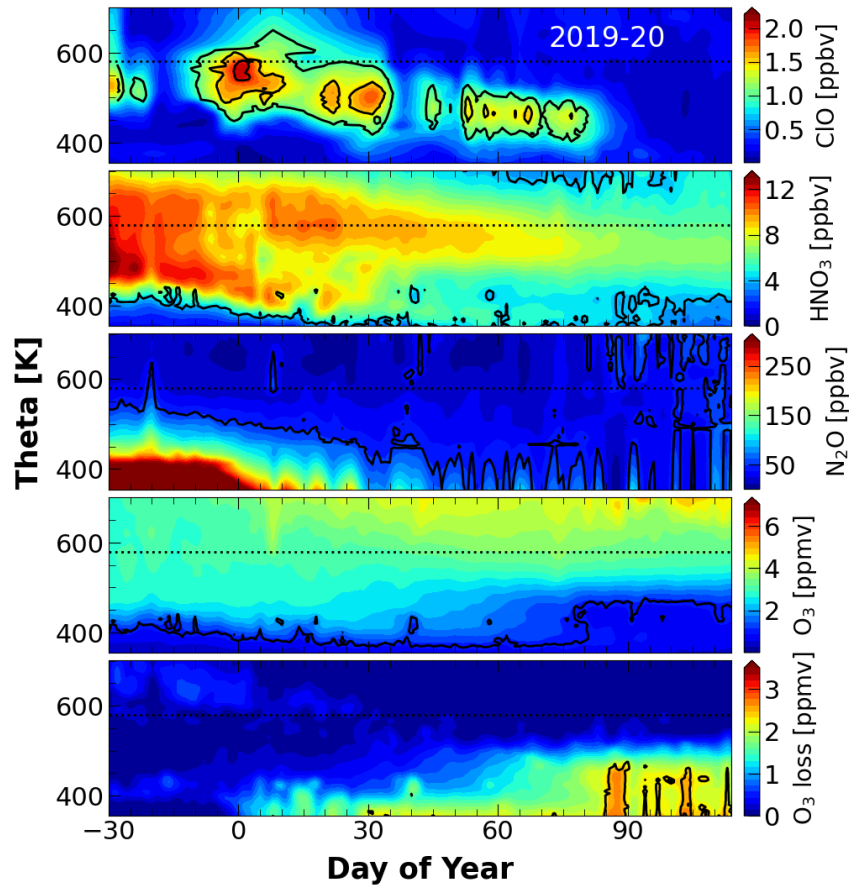
790

791

792

793

794



795

796

797

798

799

800

801

802

803

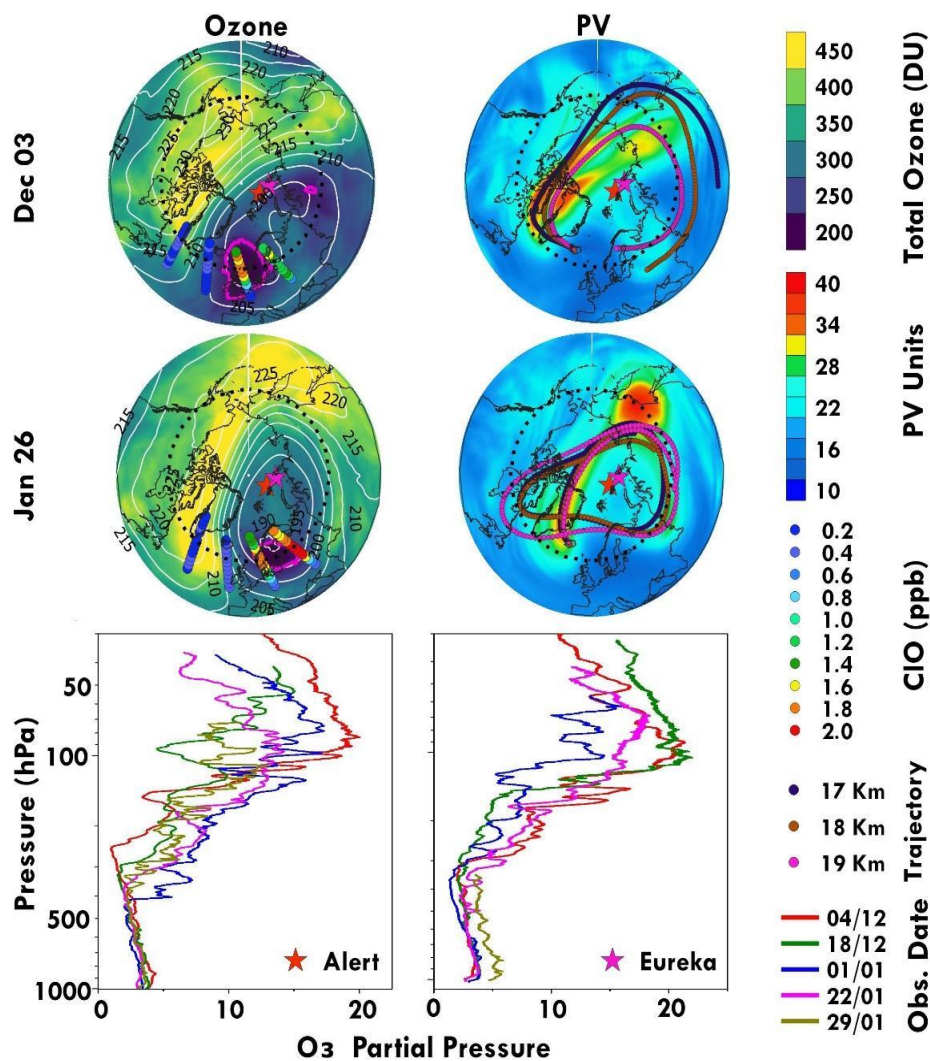
804

805

806

807

Figure 3: Ozone loss in the Arctic polar vortex in 2020. The distribution of CIO, HNO₃, N₂O and ozone (top to bottom) as measured by the Microwave Limb Sounder (MLS) for the Arctic winter 2020. The bottom panel shows the ozone loss estimated using the MLS ozone by applying the tracer descent method (see Methods and supplementary file). The vortex edge is computed in accordance with Nash et al. (1996) criterion. The vortex-sampled data are then averaged over each day and are shown.



809

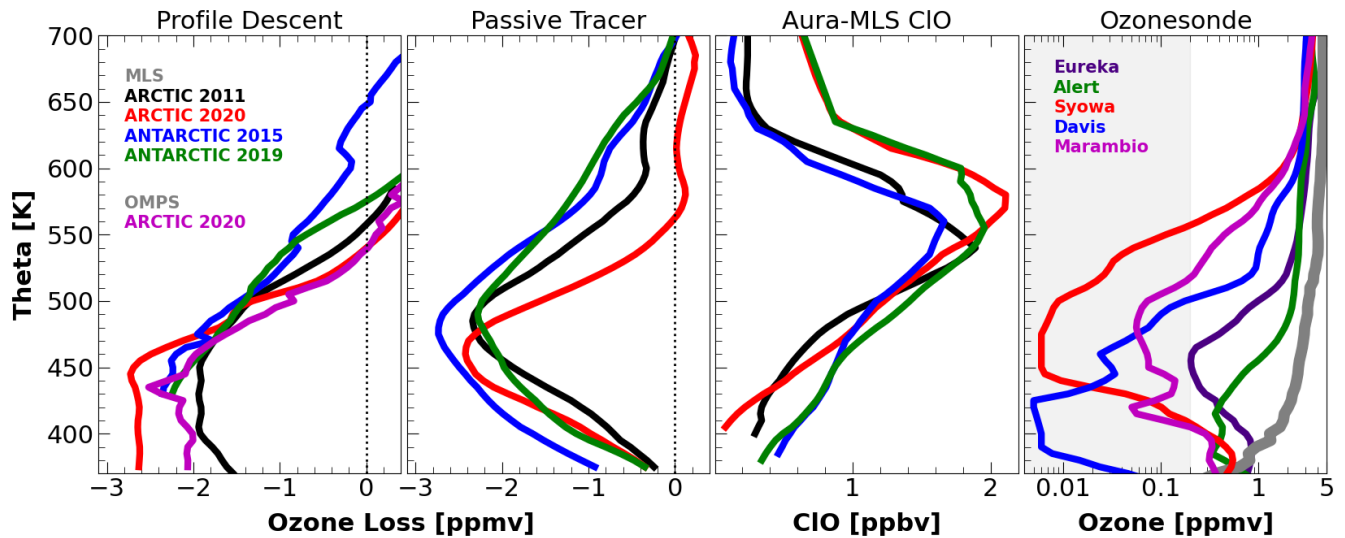
810 **Figure 4: The Arctic ozone mini-holes in December 2019 and January 2020.** The total ozone observations by Ozone
 811 Monitoring Instrument (OMI) on 03 December 2019 and 26 January 2020. The potential vorticity (PV) maps for the
 812 corresponding dates are shown on the right. The air mass trajectories computed using the HYSPLIT model at 17, 18 and 19
 813 km are also illustrated in the PV maps. The ozonesonde measurements in December and January at Alert (62.34° N, 82.49°
 814 W) and Eureka (79.99° N, 85.90° W) are illustrated in the bottom panel and are also shown in the maps as red and magenta
 815 stars, respectively.

816

817

818

819
820
821



822

823 **Figure 5: The Arctic and Antarctic Ozone Loss Saturation and Chlorine activation. Left.** The ozone loss estimated using
824 the Microwave Limb Sounder (MLS) measurements by applying the vortexdescent method for the Arctic winter 2019–2020
825 compared to the Arctic winter 2011, and the Antarctic winters 2015 and 2019. The ozone loss estimated with Ozone Mapping
826 and Profiler Suite (OMPS) measurements is also shown. **Second from the left:** The ozone loss estimated using the passive
827 tracer method for the Arctic winter 2020, and the Antarctic winters 2015 and 2019. **Second from the right:** The activated
828 profiles ClO measured by MLS for the Arctic winters 2011 and 2020, and the Antarctic winters 2015 and 2019. **The profiles**
829 **are selected for the days with peak ClO values and are averaged for three days.** **Right:** Ozonesonde measurements from
830 selected Antarctic and Arctic stations. The Antarctic ozonesonde measurements (Davis, Marambio and Syowa) from past
831 winters and the Arctic measurements (Alert and Eureka) from the Arctic winter 2020. The grey colour represents an ozone
832 profile without ozone depletion in Arctic and Antarctic. The grey-shaded region represents the ozone loss saturation threshold.
833 **The dates ozonesonde measurements are taken for 08 April 2020 (Alert) and 10 April 2020 (Eureka).**

834

835

836

837

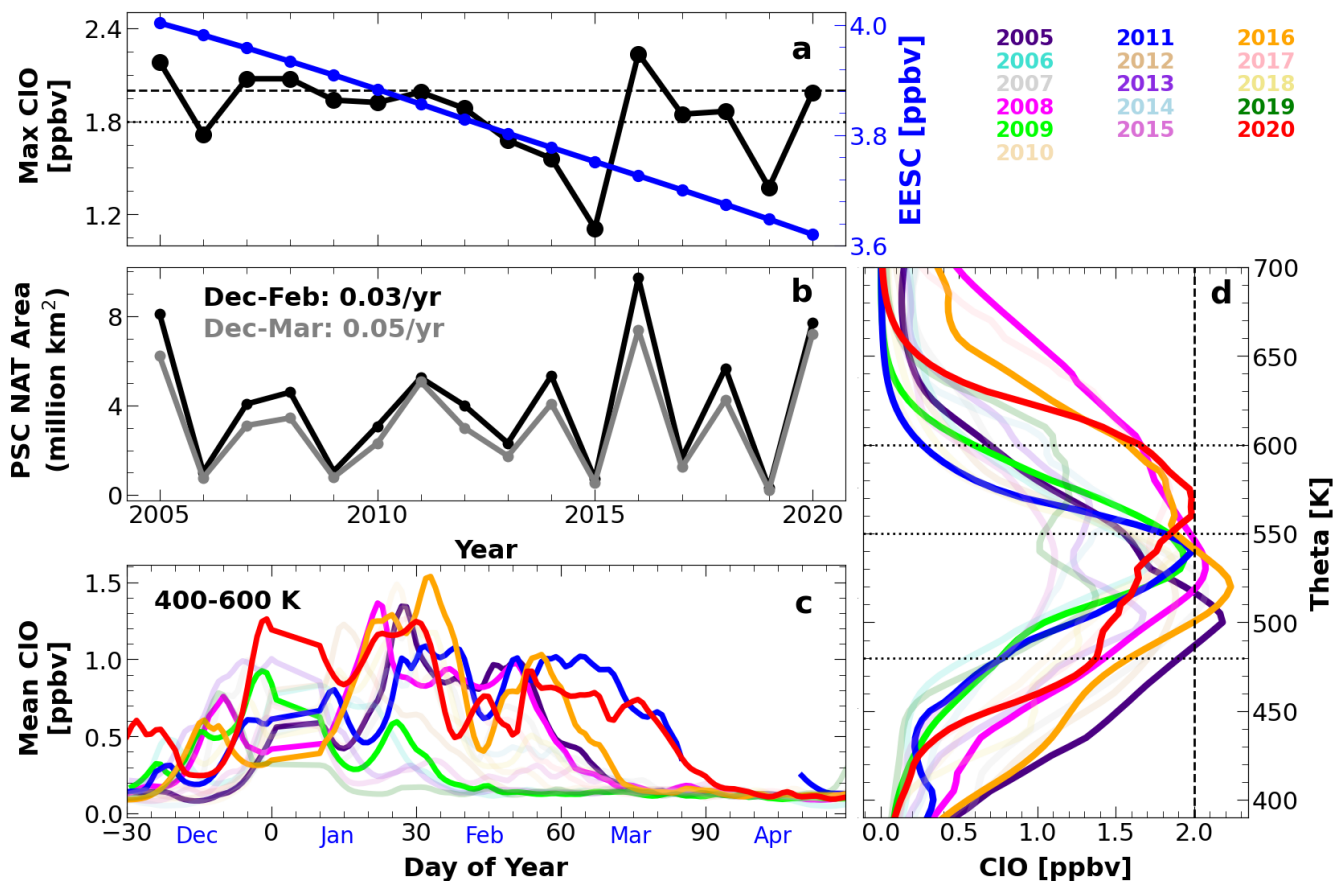
838

839

840

841

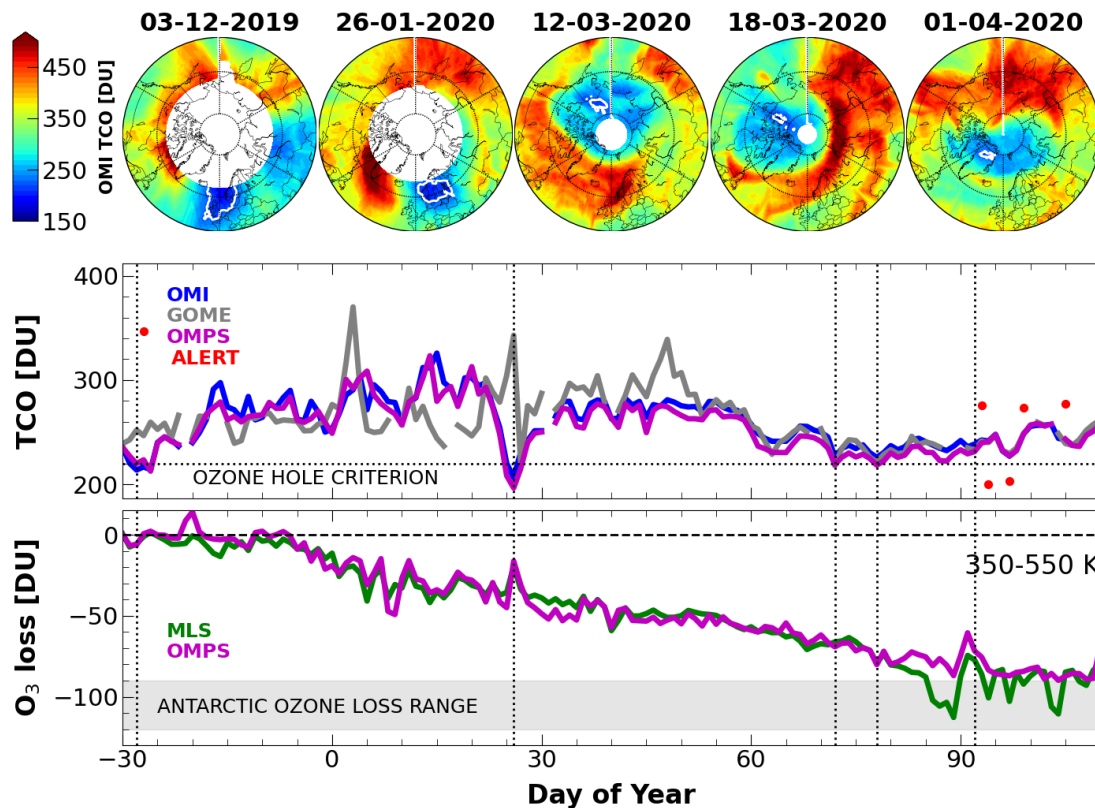
842
843
844



845
846
847
848
849
850
851
852
853
854
855
856

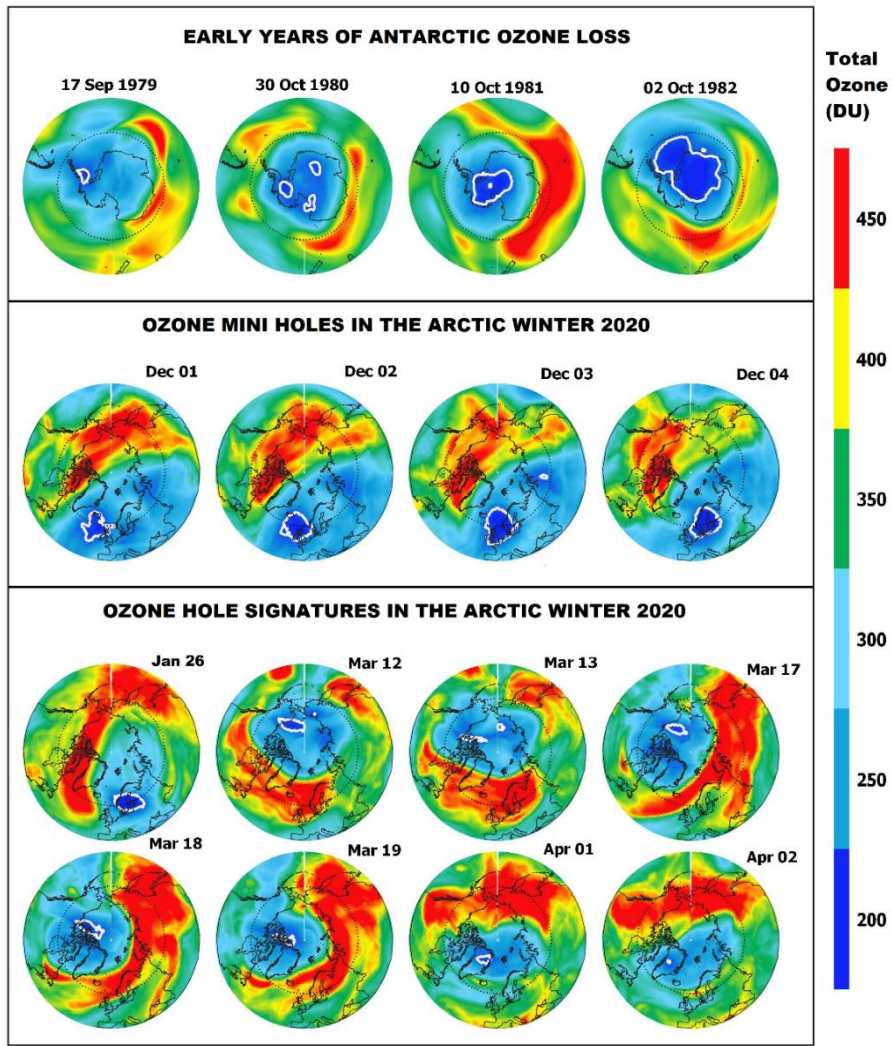
Figure 6: PSC and Chlorine activation the Arctic winters 2005–2020. (a) The temporal evolution of CIO in the Arctic winters as measured by the Microwave Limb Sounder (MLS) inside the vortex and Effective Equivalent Stratospheric Chlorine (EESC). (b) The Area of PSC averaged for the period December-February and December-March (grey) for the winter since 2005. (c) The maximum CIO measured inside the vortex in each winter from 2005 to 2020. (d) The maximum CIO profiles measured inside the vortex for Arctic winters since 2005. The high chlorine activation with high CIO values are shown in bright colours and others are faded in (a) and (c). Since the chlorine activation timing is different in different winters, the peak CIO observed between December and April/March are shown.

857
858
859
860



861
862 **Figure 7: Arctic ozone in the total column and partial column ozone. Top:** The maps of total column ozone from the OMI
863 satellite measurements in the Arctic for selected ozone hole days for the winter 2020. **Middle panel:** The lowest (5%) TCO
864 measured inside the vortex from three different satellite measurements (OMI, GOME and OMPS). The difference in total
865 column measurements is due to the difference in coverage of the measurements in the Arctic region. The ozone hole criterion
866 of 220 DU is indicated by the dotted line. The total column ozone (TCO) measurements at Alert station are also shown (red
867 solid circles). **Bottom.** The partial column ozone loss computed at the altitude range 350–550 K from the MLS and OMPS
868 measurements. The ozone loss estimated in the Antarctic winters at the same altitude range is shown as the grey -colored area.

869
870
871
872



873

874

875

876

877

878

879

Figure 8: Maps of total column ozone from MERRA -2 and OMPS satellite measurements for selected days. The Antarctic ozone hole is defined as the area below 220 DU of ozone, as demarcated by the white contour. The top panel shows the early years of the Antarctic ozone hole, the middle panel shows the ozone-mini holes driven by dynamics, and the bottom panel shows the ozone column observed in the Arctic winter 2020.

JK/REV/V05/22062021